Simultaneous detection of ascorbic acid and dopamine on nickel (II) tetra amino phthalocyanine, iron oxide decorated graphene oxide nanosheets modified glassy carbon electrode

By PRECIOUS J KHUMALO

(R152391F)

Submitted in partial fulfillment of the requirements for the degree of

Bachelor of Science Honours in Chemical Technology

Department of Chemical Technology

Faculty of Science and Technology at the

Midlands State University

Gweru

Zimbabwe

Supervisors: Dr Munyaradzi Shumba

Professor Mambo Moyo

DEDICATION

The research is dedicated to my family who has laid this foundation to fulfil my dreams and my friends for their incredible support in the course of this degree.

ACKNOWLEDGEMENTS

I would like to thank the Almighty for the gift of life and the guidance throughout my academic life. I would like to thank my supervisors Dr M. Shumba and Prof M. Moyo for their unwavering support and guidance throughout the course of this research. I would also like to thank the MSU Chemical Technology laboratory staff for their great help throughout this research. A very big thank you to some of my classmates for making the journey easier. Lastly I'd like to offer my sincerest gratitude to my parents Mr and Mrs Khumalo for believing in me and making all this possible.

ABSTRACT

Ascorbic acid and dopamine are biomolecules found in humans. They both have important functions in the body and cause numerous side effects at high concentrations. An electrochemical sensor based on nickel(II) tetra amino phthalocyanine conjugated to iron oxide doped graphene oxide nanosheets was developed.FTIR,UV- vis, cyclic voltammetry (CV) and electrochemical impedence spectroscopy (EIS) were used for characterisation of electrode modifiers.FTIR was used to ascertain that a chemical linkage between NiTAPc ,GONs and iron oxide had occurred.CV, chronoamperometry ,linear sweep and differential pulse voltammetry were used to assess the electrocatalytic oxidation of ascorbic acid and dopamine. The surface area of NiTAPc-GONs-Fe_2O_3/GCE was 0.208 cm^2. The limit of detection and limit of quantification of ascorbic acid were found to be 8.6×10^{-8} M and be 2.6×10^{-7} M respectively and LOD and LOQ for dopamine was found to be 2.58×10^{-8} M and 6.8×10^{-8} M. The catalytic rate constant was found to be $2.59 \times 10^2 M^{-1}s^{-1}$ for ascorbic acid and 1.56×10^2 $M^{-1}s^{-1}$ for dopamine. The adsorption equilibrium constant for ascorbic acid and dopamine was 6.4×10^2 M^{-1} and 8.05×10^2 M^{-1} respectively. Gibbs free energy for ascorbic acid and dopamine was found to be - 16.01 kJ and -16.57 kJ respectively. Interference studies were done and the electrode displayed the ability to detect both ascorbic acid,

dopamine and citric acid simultaneously. The electrode displayed good reproducibility with lower oxidation potentials at 0.8 V for ascorbic acid and V for dopamine. NiTAPc-GONs-Fe $_2O_3$-GCE showed high sensitivity and stability towards the detection of dopamine and ascorbic acid.

DECLARATION

I, Precious Khumalo R152391f, hereby declare that I am the sole author of this dissertation. I authorize Midlands State University to lend this dissertation to other institutions or individuals for the purpose of scholarly research.

Signature …….

Date …….

APPROVAL

This dissertation entitled **Simultaneous detection of ascorbic acid and dopamine on nickel (II) tetra amino phthalocyanine, iron oxide decorated graphene oxide nanosheets modified glassy carbon electrode** by Precious J Khumalo meets the regulations governing the award of the degree of Chemical Technology of Midlands State University, and is approved for its contribution to knowledge and literal presentation.

Supervisor……...

Date……

Table of Contents

LIST OF TABLES

LIST OF FIGURES

ABBREVIATIONS

CV	Cyclic Voltammetry
DPV	Differential Pulse Voltammetry
CA	Chronoamperometry
EIS	Electrochemical Impedance Spectroscopy
AA	Ascorbic Acid
DA	Dopamine
NiTAPc	Nickel tetra amino Phthalocyanine
GONs	Graphene oxides nanosheets
DMF	Dimethyl formaldehyde
MPc	Metallo-phthalocyanine
Pc	Phthalocyanine
GCE	Glassy carbon electrode
FTIR	Fourier Transform Infrared
UV-vis	Ultraviolet visible spectroscopy
LOD	Limit of detection
LOQ	Limit of quantification

CHAPTER ONE

1.0 INTRODUCTION

The chapter gives the background of the research carried out on the detection of ascorbic acid and dopamine using graphene oxide nanosheets, iron oxide nanoparticles and nickel phthalocyanine. It gives the aim, objectives, problem statement and justification on the simultaneous detection of ascorbic acid and dopamine using a glassy carbon electrode modified with nickel (II) tetra amino phthalocyanine conjugated to iron oxide doped graphene oxide nanosheets.

I.1 BACKGROUND

There are a variety of health benefits associated with ascorbic acid (AA),(fig 1.1a) a water soluble six-carbon lactone, also known as vitamin C. AA plays a protective role against medical conditions, such as cardiovascular disease, stroke, and cancer and there is also evidence for its function as powerful antioxidant in biological systems [1] **.** Ascorbic acid (AA) is found in both animals and plants. Ascorbic acid is involved in various biological processes for example the production of the protein collagen which is needed in the production of bones, teeth, skin and hence it is a very important nutrient for humans. AA is involved in biological processes such as the removal of free radicals which can cause diseases like Parkinson's disease and also cancer [2]. It is also an important antioxidant in the food, beverages and pharmaceutical applications. Ascorbic also has effects to humans, especially at high concentrations it can cause abdominal cramps, gut blockage or renal problems.

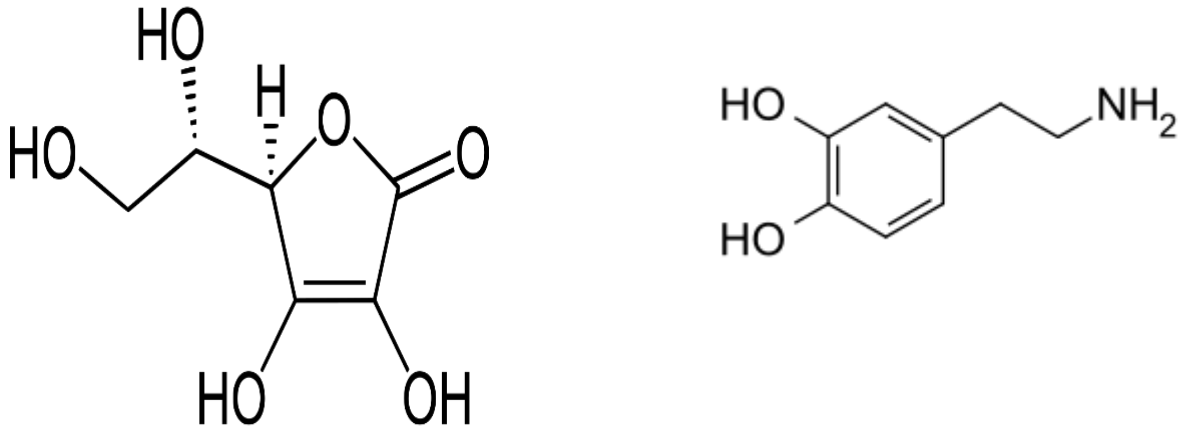

(a) (b)

Fig 1. 1 Structure of Ascorbic Acid and Dopamine [3]

Dopamine (DA), (fig 1.1b) is one of the most significant catecholamines and belongs to the family of excitatory chemical neurotransmitters. It is widely studied due to its important functions in renal, cardiovascular, hormonal and nervous systems. Because of the electroactivity of DA in the biological samples, electrochemical detection of DA has gained increasing attentions [3]. Dopamine is related to the reward system of the brain, and it has a central role in Parkinson's disease just like AA. AA also plays a role in monoamine neurotransmitters synthesis such as DA and also co-exist with it in the extra cellular fluid of the nervous system. The neurotransmitter dopamine is extensively explored by electrochemistry due to its ability to easily oxidize at a positively polarized electrode. Extreme abnormalities of DA levels can lead to brain disorders such as schizophrenia. Therefore, developing simple and rapid methods for the sensitive determination of DA and AA in routine analysis is of great importance [4, 5].

Graphene oxide nanosheets (GONs) are 2D sp^2 hybridized carbon atoms sheets that have oxygen containing functional groups that result from the oxidation of graphite. The functional groups in the GONs are carboxyl, hydroxyl, carbonyl and epoxy. The substituents of the GONs

are located on the sheet edges and the basal planes. The carboxyl and carbonyl are located at the sheet edges and the hydroxyl and epoxides are located on the basal plane. GONs have been used as chemical sensors in detecting different analytes [7] because of them being very rich in delocalized electrons due to the sp^2 hybridization of the carbon atoms. GONS can be joined to other molecules to create a new and improved composite by using their functional groups for example using the carboxyl group to a compound with an amine group and form an amide bond.GONs also have a high surface area, excellent flexibility, chemical inertness and good conductivity which makes it a good electrochemical sensor on its own [6-8].

Iron oxide nanoparticles superparamagnetic iron oxide nanoparticles with appropriate surface chemistry can be used for numerous applications in magnetic resonance imaging contrast enhancement, tissue repair, immunoassay, detoxification of biological fluids, hyperthermia, drug delivery, and cell separation [9]. They are said to be superparamagnetic because they are attracted by a magnetic field but retain no residual magnetism after the field is removed. Due to their small size and magnetic behaviour have been extensively used in several technological and biomedical applications. Iron oxide nanoparticles are preferred because of their greater saturation magnetization. In addition, the magnetite nanoparticles are very much susceptible to air oxidation and to prevent this they are coated with a surfactant [10-12].

Phthalocyanine (Pc) derivatives have a similar structure to porphyrin, but they are more stable. They have been utilized in important functional materials in many fields as colorants and optoelectronic materials [13]. Their useful properties are because of their efficient electron transfer abilities and the presence of metal centres which undergo redox reactions during electrocatalysis. The central cavity of phthalocyanines is known to be capable of accommodating 63 different elemental ions, including hydrogens [14]. A phthalocyanines containing one or two metal ions is called a metal phthalocyanines. Pcs are highly colored, planar 18 π-electron aromatic ring and have very high thermal and chemical stability [13, 14].

Different substituent groups can be introduced on the peripheries of the phthalocyanines ring and these groups can be carboxyl, amine, sulphonyl and the substituents can be used to link the Pcs to other molecules like iron oxide to form a different new chemical sensor. The beauty of Pcs is that you can tailor make the functional groups which you can use to combine to other molecules by covalent linking [15,16].

1.2 AIM OF STUDY

- Determination of the electrocatalytic behaviour of a glassy carbon electrode modified with nickel (II) tetra amino phthalocyanine conjugated to iron oxide doped graphene oxide nanosheets.

1.3 OBJECTIVES

- to synthesize nickel (II) tetra amino phthalocyanine, graphene oxide nanosheets and iron oxide nanoparticles electrode modifiers and conjugate them.
- to characterise electrode modifiers using FTIR, UV- vis, cyclic voltammetry and electrochemical impedance spectroscopy.
- to determine optimum pH for analytes ascorbic acid and dopamine using the best electrode.
- to detect analytes using cyclic voltammetry, differential pulse voltammetry, chronoamperometry, linear sweep voltammetry and electrochemical impedance spectroscopy using the best electrode.
- to carry out interference, stability and reproducibility studies of the developed electrode towards detection of ascorbic acid and dopamine.

1.4 PROBLEM STATEMENT

Ascorbic acid is a very important vitamin is found in both plants and animals. It can also be found in diet and is used as an antioxidant in the food industry and pharmaceutical formulations. It is used to treat different disease such as atherosclerosis and infertility. Deficiency of ascorbic acid can cause scurvy and excess AA causes abdominal cramps, nausea and gut blockage. Its absence in the nervous system can also result in brain diseases like parkinson's disease since it is responsible for the removal of free radicals which cause the disease. Due to the importance and negative effects of AA its analysis in solution is important especially in the medical field in checking its concentration levels [4,17] .

DA is also a hormone that is related to many important functions in the human brain and body. It is closely related to brain functions, such as motivation, sleep, attention, and learning. The malfunction of the dopamine system results in several brain diseases, such as attention deficit, hyperactivity disorder, restless legs syndrome, schizophrenia, Parkinson's, and Alzheimer's disease [5,18]. The DA concentration is quite low in the nerve cell, extracellular fluid of the central nervous system and cerebrospinal fluid. Several methods have been implemented to detect DA and AA, such as electrogenerated chemiluminescence, colorimetry, capillary electrophoresis, fluorescence spectrometry, and high-performance liquid chromatography [3]. Challenges associated with the other techniques are that they are very expensive, time consuming, they need a lot of skill in the operation and sometimes suffer from low detection limit.A lot of attention has been paid to fluorescence spectrometry due to its simplicity, easiness, and high accuracy in the detection of DA, especially at low concentration levels. However, the detection of DA by fluorescence in biological matrices usually suffers from interference by ascorbic acid (AA) since they coexist in the extra cellular fluid of the nervous system. Thus, it is important to design a new method for the determination of DA in the presence of AA with high selectivity and sensitivity [5]. Consequently a cheaper, faster,easier

to use, low power consuming, miniaturizable size, user friendly and on site analytical device suitable to compliment or substitute for these classical methods is developed in form of NiTAPc-GONs-Fe_2O_3 electrochemical sensor for the detection and quantitative determination of AA and DA.

1.5 JUSTIFICATION

Graphene oxide has been used as a modifier on its own and has shown to be a good one because of its delocalized electrons which result from sp^2 hybridization. The use of phthalocyanines as modifiers has also received great attention and just like graphene oxide nanosheets they have shown to be very good modifiers. The covalent combination of nickel tetra amino phthalocyanine and graphene oxide nanosheets using their substituents will create a very good sensor that will combine the effects of the Pcs and GONs and improve electron transfer, which is the primary aim when making electrode modifiers [19, 20]. Electrochemical techniques particularly are being used as alternatives for the detection of ascorbic acid and dopamine because of the improvement in sensitivity, specificity, simplicity and rapidity [6].Inorder to improve the detection of ascorbic acid and dopamine even at very low concentrations iron oxide, graphene oxide nanosheets and nickel phthalocyanines have be used as electrode modifiers. Iron oxide nanoparticles are superparamagnetic therefore are preferred because of their saturation magnetization for detection of DA and AA [10, 12, 21]. In addition to the large surface area iron oxide nanoparticles are used because of their low cost, non-toxicity, eco-friendly and good biocompatibility [22]. NiTAPc was chosen due to the presence of amino groups on the periphery which can form an amide bond with the carboxylic acid group of the GONs.NiPc complexes are also well known electrocatalysts [23].Nickel tetra amino phthalocyanine (NiTAPc) is a member of the metallo-phthalocyanine family known for their excellent redox chemistries and applications in various technologies such as in sensing and electrocatalysis. The efficient combination of GONs with NiTAPc is expected to prevent

restacking and also improve the conductivity of the composite thereby leading to an improved electrochemical performance of the electrode material [24].

CHAPTER TWO

Literature Review

2.0 Introduction

This chapter gives detailed information of ascorbic acid and dopamine and also the detailed information on the modifiers components that are used to make a chemical sensor that is used to detect these analytes. It also gives information about the electrochemical techniques used in this research.

2.1 Dopamine

Dopamine (3, 4-dihydroxyphenethylamine) (fig 2.1) is a neurotransmitter of the catecholamine family, which is widely distributed in the central nervous system of animals for message transfer from one neuron to another neuron. It is derived from l-tyrosine by a series of biochemical reactions using tyrosine hydroxylase and decarboxylase, and it is the precursor to norepinephrine (noradrenaline) and epinephrine (adrenalin). DA is also a hormone that is related to many important functions in the human brain and body. It is closely related to brain functions, such as motivation, sleep, attention, and learning. The malfunction of the dopamine system results in several brain diseases, such as attention deficit hyperactivity disorder, restless legs syndrome, schizophrenia, Parkinson's, and Alzheimer's disease. It has been widely studied due to its important functions in renal, cardiovascular, hormonal and nervous systems [17]. Because of the electroactivity of DA in the biological samples, electrochemical detection of DA has gained increasing attentions. Electrochemical determination of DA by direct oxidation using the commonly employed electrodes is difficult, mainly due to cooxidation of

ascorbic acid (AA) at a potential similar to that of DA. Many efforts have been made to tackle the problem, using a variety of modified electrodes [25] .

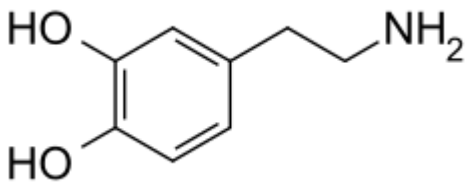

Fig 2. 1 Structure of dopamine [17]

2.2 Ascorbic acid

Ascorbic acid (AA) (fig 2.2) also known as vitamin C is a water-soluble biomolecule found in both animals and plants. AA is also present in vegetables, beverages, food, and pharmaceutical products. It is involved in immune response activation and in wound-healing osteogenesis. It is also involved in biological processes like the removal of free radicals which can cause diseases like the Parkinson's disease, therefore its presence in optimum amounts is very vital in the human body. Adequate amounts of ascorbic acid is very important in protecting the skin and prevention of scurvy [20,26]. Different diseases can be treated using vitamin C for example the Alzheimer's disease, atherosclerosis and it can also be used in dealing with infertility. In recent years using ascorbic acid has been known to be a non-toxic way to treat cancer, it has been occasionally used in place of chemotherapy [20]. The reason being that ascorbic acid damages the DNA of cancer cells but not the normal cells unlike chemotherapy which damages both cancerous cells and normal cells. It is lethal to cells because it chemically resembles glucose and it inhibits the enzyme that the cancer cells need to spread [1,2,27]. If ascorbic acid is in excess it can cause abdominal cramps, gut blockage, gastric irritation, renal problem which is caused by oxalic acid which is one of its metabolites [28].

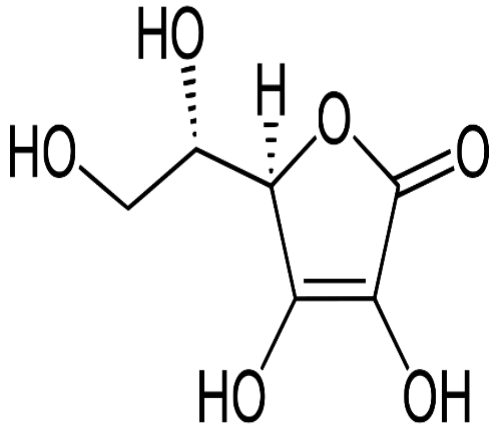

Fig 2. 2 Structure of AA [2]

2.3 Phthalocyanines

2.3.1 Discovery

Phthalocyanines are planar macrocyclic aromatic compounds which possess an 18π electron system. Phthalocyanine derivatives, which have a similar structure to porphyrin, have been utilized in important functional materials in many fields. Their useful properties are attributed to their efficient electron transfer abilities. The central cavity of phthalocyanines is known to be capable of accommodating 63 different elemental ions, including hydrogens. A phthalocyanine containing one or two metal ions is called a metal phthalocyanine.The structure is made up of 4 isoindoline units joined by four azo nitrogens and their structure is similar to that of naturally occurring porphyrins. Metal-free phthalocyanine was obtained by accident for the first time in 1907 as a by-product during the preparation of 2-cyanobemzamide. Twenty years after this discovery, copper phthalocyanine was synthesized by Disbach and his coworker from 1,2-dibromobenzene in 1927 Linstead and his coworkers prepared several metallophthalocyanines by developing synthetic methods and elucidated the structure of phthalocyanine. The name phthalocyanine was first used by Linstead to describe both its origin

from phthalic anhydride (phthalo) and its beautiful colour which was similar to cyanine dyes [13, 14, 29, 30].

2.3.2 Structure of Pcs

Phthalocyanines are more stable analogs of the porphyrins and are more commonly used in industry. Phthalocyanine molecules have a conjugated system of 18 π electrons and possess a very high thermal and chemical stability. The structure of the phthalocyanine ring resembles the naturally occurring porphyrins with the only basic difference being the aza groups instead of methine corner links. Phthalocyanine offers up to sixteen sites for substitution and the established numbering system for the basic ring system. Like the porphyrins, Pcs are a class of macrocyclic compounds have bivalent, tetradentade, planar, 18 π-conjugated electron aromatic ring systems. In contrast, Pcs are composed of four pyrrole units linked by four aza (—N=C—) groups at the α-carbon of pyrrole unit and they have four aza bridges and four phenylene rings There are various metal-free and metallo-tetrapyrolles. MTPs are highly stable macrocyclic π-systems that display interesting properties that make them potential candidates for various application [14, 29, 30, 31].

2.3.3 Application of Phthalocyanines complexes

Phthalocyanines complexes were initially used as dyes and pigments due to their intensive colour however they might be used in many applications such as photocopying, laser printing, oil screening, molecular semiconductors, photosensitizers in antitumious and infrared devices. Phthalocyanines complexes are used in a number of applications because of their increased stability, architectural flexibility, diverse coordination properties and improved spectroscopic characteristics [30]. They are increasing interest in application in nonlinear optics xerography as photoconductors, solar energy conversion and as the active components of gas sensor.

Phthalocyanines have a strong optical absorbance in the red and near IR portions of the electromagnetic spectrum and are stable under a wide range of thermal and electrochemical condition. The main contributor for its electro catalytic properties lies on the binding behavior of the metal center to interact with axial ligand sphere. Metallophthalocyanines have the ability to gain or lose many electrons and can still retain their molecular structure and stability due to their dual donor π acceptor function. This property accounts for their ability to exhibit electrocatalytic activity [13, 29]. Unsubstituted phthalocyanines exhibit very low solubility in most of commonly used organic solvents as a result of strong π- π interactions of phthalocyanine macro rings in crystalline state. The electro catalytic activity of the modifier is mediated by the metal or the ring. The established mechanism of the electro catalyst by MPcs is believed to be a two-step process initiated by the electrochemical oxidation of the central metal or the ring, followed by the electron transfer from the species being oxidized to the metal, regenerating the initial catalyst. Mechanism for the metal based electro catalyst oxidation of the analyte.

$$M^{II}P^{c-2} \longrightarrow M^{III}P^{c-2} + e^{-} \quad (2.1)$$

$$M^{III}P^{c-2} + C \longrightarrow M^{II}P^{c-2} + C_{Oxidised} \quad (2.2)$$

Were C is the analyte of interest and $C_{Oxidised}$ is the oxidation product of C [32]

2.3.4 Methods of synthesis of phthalocyanine

The various 1.2–disubstituted benzene precursor have been employed successfully for phthalocyanine synthesis i.e. phthalonitriles, isoindolines, phthalic acid, phthalimides, phthalic acid and anhydride derivatives, 1.2- dibromobenzenes and 2 cyanobenzamide as shown in (fig 2.3). Depending on the temperature, base, nature of the substituents, solvent, choice of

precursor, metal salt and the metal to be inserted into the macrocycle with wide range of conditions have been utilised.

I. Reaction of phthalonitrile with metal or metal salt in a high boiling liquid like nitrobenzene or quinoline. In this reaction phthalonitrile and metal chloride with mole ratio 4:1 is heated to 180-190 ºC for 2 h in quinoline or mixture of quinoline and trichlorobenzene. Cobalt, nickel, chromium, iron, lead and titatinum phthalocyanine have been synthesised by this method. Direct method of synthesis of metal – free phthalocyanine (H_2Pc) involves heating of phthalonitrile with a base (NH_3) in a solvent (1-pentanol).

II. Reaction of phthalic acid or phthalic anhydride with urea and metal salts in the presence of a catalyst or phthalimide with a metal salt in the presence of catalyst. A stoichiometric mixture of phthalic anhydride, a metal salt, urea and catalyst is heated at 170-200 ºC for 4 h in medium such as nitrobenzene, chlorobenzene .

III. Reaction of phthalocyanine or liable metal phthalocyanine with a metal forming a more stable Pc.

IV. Reaction of o-cyanobenzamide with a metal.

V. Polymeric phthalocyanine are synthesised by starting with a tetrafunctional benzene 1.2.4.5- tetracyanobenzene or pyrometallic.

VI. The phthalonitrile route is expensive but gives high purity products thus this method is mostly used for technological application where high purity and high quality is required [33, 34].

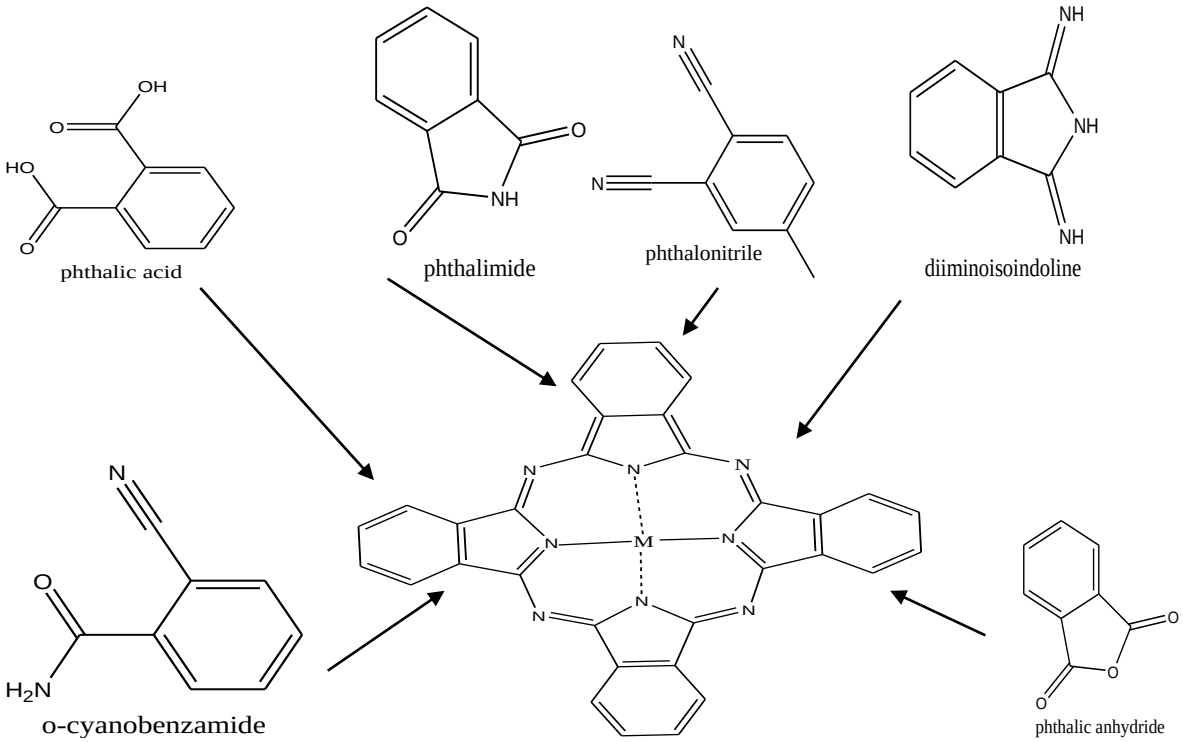

Fig 2. 3 Synthesis methods for metallophthalocyanines

2.3.5 Tetra-substituted Pcs

Substituents can be introduced directly onto the existing Pc ring, e.g. sulphonation or by using monosubstituted Pc precursors as shown in (fig 2.3) for nickel (II) tetra amino phthalocyanine. Pcs have 16 possible positions of substitution around the ring, substitution on one α- position or one β-position on the four phenyl groups of the Pc ring produces isomeric tetra-substituted Pcs with reduced aggregation tendencies. Polar substituents such as sodium salts of sulphonic acid, carboxylic acid or phosphonic acid groups provide water-soluble MPcs. In this study, focus is on peripherally tetra-substituted MPcs, using carboxylic acid and amine groups that

can be joined together and be further derivatized with graphene oxide for use in electro catalysis [32].

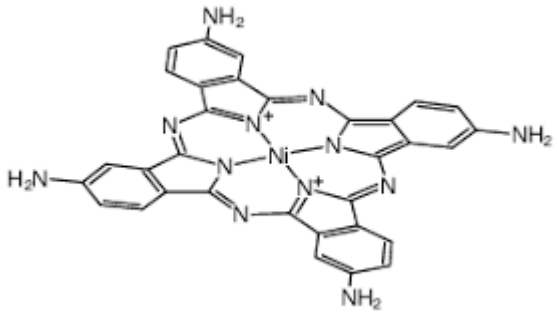

Fig 2. 4 Structure of nickel (II) tetra amino phthalocyanine [24]

2.3.6 Electrochemical properties of metallophthalocyanines

Electrochemistry of MPcs complexes occurs at the Pc ring or at the central metal ion provided the metal ion is electroactive and its orbitals lies between the HOMO and LUMO energy gap themselves as excellent electrocatalysts especially. The catalytic effect of the MPcs can be seen when the Pc has been immobilised onto the electrode surface and oxidation and reduction analysed electrochemically. The oxidation and reduction can either occur at the central metal cation or the Pc ring. However, it is the central metal in the Pc that is involved in the reaction such as metal – ligand interaction, electronic structure and the majority of the redox reactions [35] .Electrocatalyst is a metal rich catalyst used to promote the efficiency of a half reaction of an electrochemical reaction. This promotion of electrochemical reaction can be accomplished in one of the three ways by lowering of the applied potentials to accessible values, increase in peak current densities or increasing in slope, improved peak slopes [36]. The effectiveness of MPc containing transition metals as catalysts lies in the fact that they have unpaired electrons and unfilled d orbitals that are available to form bonds with the analyte. The most commonly used electroactive metal ions for MPcs are Co, Fe and Mn.The potentials at which these redox

reaction occur can be influenced by the nature of the substituents on the Pc ring, oxidation state of the central metal ion and if present the axial ligand and the solvent used. MPc exists as dianion (MPc^{-2}) in their neutral form. The oxidation process which is the successive removal of two electrons from the HOMO (a_1u) of the neutral MPc^{-2} results in the formation of the MPc^{-1} and MPc^{0} species. Reduction process is successive addition of electrons to the LUMO of the MPc^{-2} results in the formation of MPc^{-3}, MPc^{-4}, and MPc^{-5} and MPc^{-6} species. Metal oxidation and reduction is characterized by a shift in the Q band without much reduction in intensity [13, 30]

2.4 Iron Oxide

Iron oxide nanoparticles are mostly used as magnetic particles in ferrofluids due to their high saturation magnetization and high magnetic susceptibility. The magnetite (Fe_2O_3) particles are preferred because of their greater saturation magnetization. The nanoparticles need to be stabilized in the carrier liquid because they tend to agglomerate due to Van der Waals forces. In addition, the magnetite nanoparticles are very much susceptible to air oxidation. In order to prevent the possible air oxidation as well as agglomeration, the Fe_2O_3 nanoparticles are coated with a surfactant or a polymer. Also once the dispersing agent is adsorbed on the iron oxide particles, the number of accessible sites for further crystal growth is reduced to keep the particle size small. Superparamagnetic iron oxide nanoparticles with appropriate surface chemistry can be used for numerous in vivo applications, such as magnetic resonance imaging contrast enhancement, tissue repair, immunoassay, detoxification of biological fluids, hyperthermia, drug delivery, and cell separation. All of these biomedical applications require that the nanoparticles have high magnetization values, a size smaller than 100 nm and a narrow particle size distribution. These applications also need peculiar surface coating of the magnetic particles which has to be nontoxic and biocompatible and must also allow for a targetable delivery with

particle localization in a specific area. Such magnetic nanoparticles can bind to drugs, proteins, enzymes, antibodies, or nucleotides and can be directed to an organ, tissue, or tumour using an external magnetic field [9,11,37].

2.5 Graphene Oxide

The study of carbon nanostructures is very wide due to their unrivalled properties and a wide range of applications. Among the different species of carbon, graphene is one of the most talked about in the present era due to its remarkably excellent properties. Graphene Oxide (fig 2.5) is defined as a single layer of hexagonally arranged carbon atoms which form a polycyclic hydrocarbon network which is arranged in a planar condensed ring system [6,38]. It contains a two-dimensional structure of sp^2 hybridized carbon which exhibits very good electrochemical, thermal and mechanical properties. The functional groups in the GONS are carboxyl, hydroxyl, carbonyl and epoxy. The substituents of the GONS are located on the sheet edges and the basal planes. The carboxyl and carbonyl are located at the sheet edges and the hydroxyl and epoxides are located on the basal plane. GONS have been used as chemical sensors in detecting different analytes because of them being very rich in delocalized electrons due to the sp^2 hybridization of the carbon atoms [39, 40]

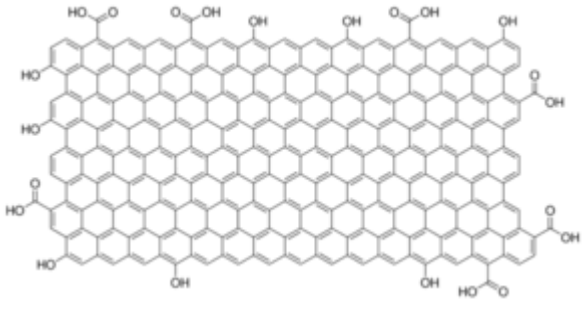

Fig 2. 5 Structure of grapheme oxide nanosheets [38]

2.6 Surface characterization

There are various methods used for the characterisation of Pc and the modified electrode surface and such methods include Fourier Infrared red spectroscopy and Ultra violet/visible spectroscopy.

2.7 Fourier Infrared red spectroscopy

This technique involves identifying chemicals that are either organic or inorganic compounds or the presence of certain functional groups in the molecule. Fourier Infrared red spectrum provides information regarding the identity, quality, chemical bonding of the atoms caused by the vibration between the atomic bands represented by the absorption band of the sample. Advantages of FTIR over other dispersive techniques are that it is highly sensitive due the high signal to noise ratio, simple and high rate of data generation [41, 42]

2.8 Ultra-Visible spectroscopy

This technique shows a number of characteristic absorption in the visible and ultraviolet regions. The isolated band in the red end of the visible region, which appears around 670-800 nm region is known as the Q band [43].It is an analytical technique which applies to both quantitative and qualitative analysis. The UV spectrum of Pc is understood through the use of Goutermans four orbital model (fig 2.6), a model based on a linear combination of aromatic orbitals.

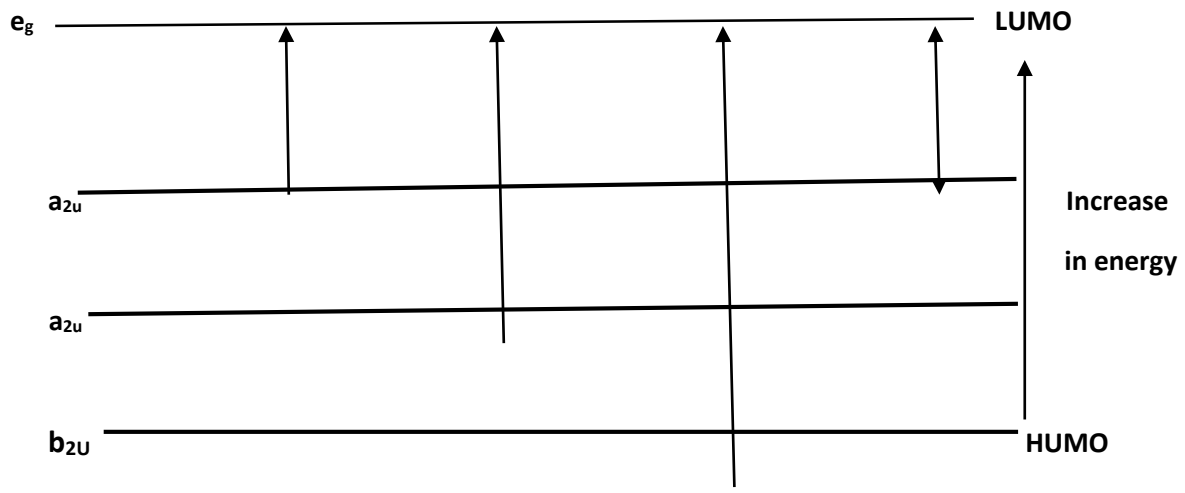

Fig 2. 6: Diagrammatic representation of the origin of the UV-Vis Q and B band.

The models interprets the spectrum in terms of the transition between the two highest occupied molecular orbitals (HOMO) which are a_1u (π) followed by the a_2u (π) to be the lowest unoccupied molecular orbital (LUMO) which is doubly degenerate e_g. The Q band originate from the π- π^* electronic transition from HOMO to LUMO of the PC ring involving a_1u and e_g orbitals. It is also used where the B band are thoroughly analysed [44, 45, 46].

2.9 Cyclic voltammetry

Cyclic voltammetry (CV) is an electroanalytical technique which has been effectively applied for analytical, thermodynamic redox reaction, reversibility, mechanistic and kinetic of heterogeneous electron transfer studies. It is the most effective analytical technique available for the study of redox systems that provides an excellent and convenient tool to determine whether an electrochemical reaction is diffusion or kinetically controlled. Apart from its use in quantitative determinations, CV it is widely used for the study of redox process, understanding reaction intermediates and for obtaining stability of reaction products [47].It also provides an effective way of determining the amount of modifier deposited on the electrode surface. The surface coverage is determined by cycling the electrode with the appropriate potential window in a solution that contains a supporting electrolyte and determining the area under the oxidation

or reduction wave [48]. Surface area for the modified electrode is determined by using the $Fe(CN)_6^{3-/4-}$ redox system and the Randles Sevcik equation. It offers a rapid location of redox potentials of electroactive species. It has found a wide range of applications in industrial quality control, geology, material chemistry, biomedical analysis and environmental monitoring. In this research modified electrode is used to develop an analytical method for the electrocatalytic detection of hydrogen peroxide. Cyclic voltammetry monitors redox behaviour of hydrogen peroxide within a wide potential range. The working electrode is where the electrochemical reaction of interest takes place and it provides high signal to noise ratio. In cyclic voltammetry studies, the working electrode potential is ramped linearly versus time using a triangular potential waveform from the initial value to some predetermined final value followed by reversing the scan. To obtain a cyclic voltammogram as illustrated in (fig 2.7), the current at the working electrode in an unstirred solution is measured during the potential scan. The potential is applied between the reference electrode and the working electrode and the current is measured between the working electrode and the counter electrode. The controlling potential that is useful across the working electrode and the reference electrode is called the excitation signal. These data are then plotted as current (i) vs. potential (E).The peak height (I_P) and peak potential E_p are dependent on the state of the GCE surface [53-55].

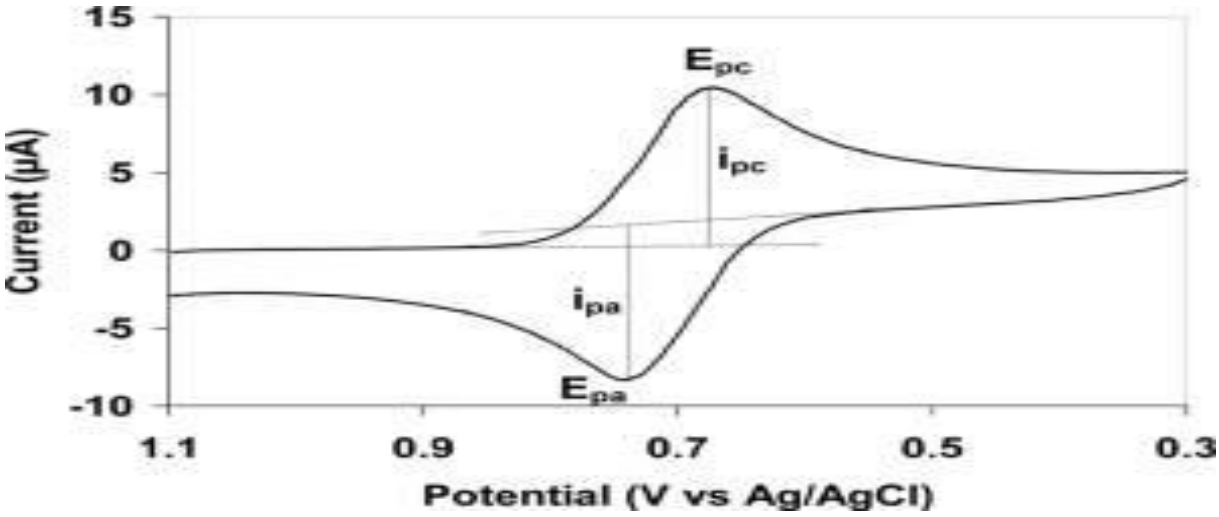

Fig 2. 7 Cyclic voltammetry

The current will increase as the potential reaches the reduction potential of the analyte, but then falls off as the concentration of the analyte increases. If the redox couple is reversible then when the applied potential is reversed, it will reach the potential that will reoxidize the product formed in the first reduction reaction and produce a current of reverse polarity from the forward scan. Cyclic voltammetry processes are either reversible, quasi reversible or irreversible depending on the nature of the reaction.

2.9.1 Reversible process

A reversible process is the one in which the electron transfer process is rapid and the electroactive oxidised species in the forward scan is in equilibrium with the electroactive reduced species in the reverse scan. Reversibility is a direct and straight forward means of probing the stability of an electroactive species. To stimulate the cyclic voltammetry a simple one electron transfer reaction with Bulter Volmer kinetics is considered using Equation:

$$Ox + ne \longrightarrow Rd \qquad (2.3)$$

where n is the number of electrons transferred per mole of the electro active species. At 25 ^{o}C , the peak current in the reversible systems for the forward scan is given by Randles-Sevcik relatively Equation.

$$I_{pc} = 2.69\times10^{8}\, n^{3/2} A D^{1/4} v^{1/2} C \qquad (2.4)$$

where I_{pc}-peak current, A- electrode area, *v*- scan rates, D –diffusion coefficient m/s, C-concentration and n – number of electrons involved. A linear plot of I_p vs $v^{1/2}$ indicates that currents are controlled by planar diffusion to electrode surface. The potential where the current is half of its limiting value is known as half wave potential ($E_{1/2}$) which is the average of the two peak potentials. The formal reduction potential E^{o} for a reversible couple is the mean of E_{pa} and E_{pc} and l_{pa} and $l_{pc.}$

$$E_o = \frac{E_{pa} - E_{pc}}{2} \qquad (2.5)$$

The number of the electrons involved in the redox reaction for reversible couple is related to the difference of peak potentials.

$$E_{pc} - E_{pa} = \frac{57\ mV}{n} \qquad (2.6) \qquad [55,56]$$

2.9.2 Irreversible process

It is a process whereby the reaction goes one way, the most common is when only a single oxidation or reduction peak with a weak or no reverse peak. Irreversible processes are a result of slow electron transfer or chemical reactions at the surface of the working electrode. Totally irreversible systems are characterized by a shift of a peak potential E_{pa} and $E_{pc,}$ with an increase in scan rate [57].

2.9.3 Linear scan voltammetry

Voltammetric method in which the potential applied to the working electrode is varied linearly in time. The potential of the working is ramped from an initial potential applied E_i to final potential E_f. With a linear potential ramp the faradaic current is found to increase at higher scan rate due to the increase in flux of electro active material at the electrode [58] .

2.9.4 Glassy carbon electrode

The glassy carbon electrode material is homogenous and share the basic structure of a six member aromatic ring and sp^2 bonding. The high degree of delocalization of the π electrons together with the weak van der Waals forces provides for its good electrical conductivity. Glassy carbon electrode is a solid isotropic material composed of thin convoluting micro fibrils that interlock to form strong interfibrillar bonds. Glassy carbon electrode has been used due to their low background current, high electrical conductivity, high stability, rich chemistry, chemical inertness and low cost. They have exceptional mechanical electrical properties, highly chemically stable, have a large specific area. GCE are generally pretreated either electrochemically or mechanically to obtain a reproducible electrode surface [59].

2.10 Modified electrodes

Electrochemical sensors have been proven as simple analytical method with remarkable detection sensitivity, reproducibility and ease of miniaturation rather than an instrumental analysis method. Direct voltammetry of a substance at a bare electrode has led to electrode fouling by unwanted precipitation, contamination the slow electrochemical reaction rates of some species that require the application of a high over potential and the oxidation product strongly adsorb on the electrode [59]. Chemical modified electrodes have found numerous

important applications in solar energy conversion, molecular electronics, electrochemical sensors, heterogeneous electrocatalysis, solar energy conversion, energy storage, information storage, corrosion protection and electro analysis. For electro analytical purpose and electro catalysis, a chemically modified electrode is used to amplify the detection signal. Several different chemically modified electrodes have been fabricated for electro analysis including mediators immobilised in a monolayer film, multilayer films [60]. Catalyzed redox reaction of an analyte result in catalytic currents indicating a substantial chemical amplification of the detection signal. Advantages of modifying glassy electrode carbon is that they increase the selectivity, sensitivity, reproducibility and the stability of the electrode. There is creation of large specific surface area, high void volume and also the electrode becomes resistance to high temperature in non-oxidizing environment [61].

Modification of the electrode surface can be done through several modification methods such as chemisorptions, addition of redox polymers, mechanical attachment, solvent casting, ion exchange chemical reactions, composite formation or polymer coating [54]. Polymer clays, organic material enzymes, biochemical compound, metal cyanometallates, phthalocyanines, carbon nanotubes and metal oxides have been used as mediator for the fabrication of the modified electrode [62].

2.11 Electrochemical Impedance spectroscopy

Impedance spectroscopy methods are based on the perturbation of the electrochemical cell with a signal of a small magnitude. Electrochemical Impedance spectroscopy (EIS) is used to characterize the deposition of self-monolayers or polymers on the electrode surface, to probe the redox and structural features of a surface of species. One way of modeling electrochemical process at the electrode solution interface involves comparison of the electrochemical process to equivalent electrical circuit containing combination of resistance and capacitance. In

Randles circuit, it is assumed that the resistance to electron transfer and the Warburg impedance are both parallel to the interfacial capacity. This parallel combination of R and C gives rise to a semicircle in the complex plane plot of Z against Z^{I} (Nyquist plot). In case of very fast electron transfer process, the impedance spectrum could include only the linear part, whereas a very slow electron transfer step results in a big semi-circle region that does not have a straight line as shown in (fig 2.8). The semi-circle diameter is equal to $R_{CT.}$ The semicircle diameter in the Nyquist plot is expected to be smaller when the GCE is modified with than when it is bare [58].

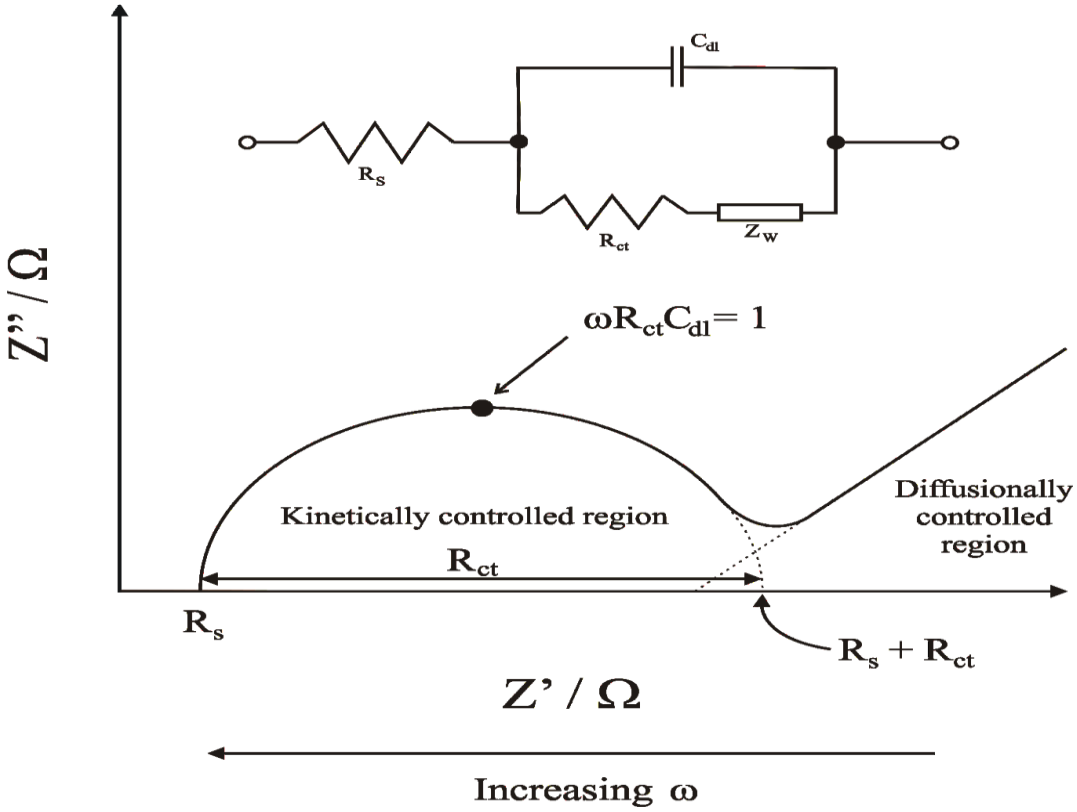

Fig 2. 8 Nyquist Plot [58]

2.12 Chronoamperometry

Chronoamperometry (CA), another commonly used electroanalytical technique, is a useful tool for determining diffusion coefficients and for investigating kinetics and mechanisms. Unlike the CV technique, CA can yield this information in a single experiment. When a potential step large enough to cause an electrochemical reaction is applied to an electrode, the current changes with time. The study of this current response as a function of time is called chronoamperometry (CA) and a plot of current against time called a chronoamperogram is made as shown in (fig 2.9) [58]

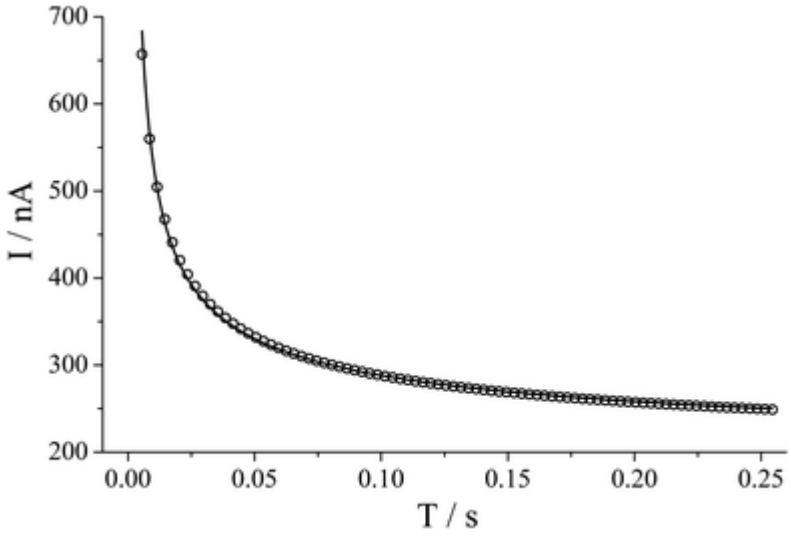

Fig 2. 9 A chronoamperogram [62]

The most useful equation in chronoamperometry is the Cottrell equation, which describes the observed current, at any time following a large forward potential step in a reversible redox reaction as a function of $t^{-1/2}$.

$$i(t) = \frac{nFACD^{1/2}}{\pi^{1/2}t^{1/2}} = kt^{1/2} \qquad (2.7)$$

Where i (t) = current, N= number of electron, F =Faraday's constant, C =bulk concentration of electroactive species, D=diffusion coefficient, T= lapsed time (s), K= catalytic rate constant $M^{-1}s^{-1}$ [62, 63].

2.6.4 Differential Pulse Voltammetry

Differential pulse voltammetry (DPV) measures the difference between two currents just before the end of the pulse and just before its application. The base potential is implemented in a staircase and the pulse is a factor of 10 or shorter than the pulse of the staircase waveform [65].The difference between the two sampled currents is plotted against the staircase potential leading to a peak shaped waveform. At potential around the redox potential, the difference current reaches a maximum, and decreases to zero as the current becomes diffusion controlled. The current response is therefore a symmetric peak as shown below.

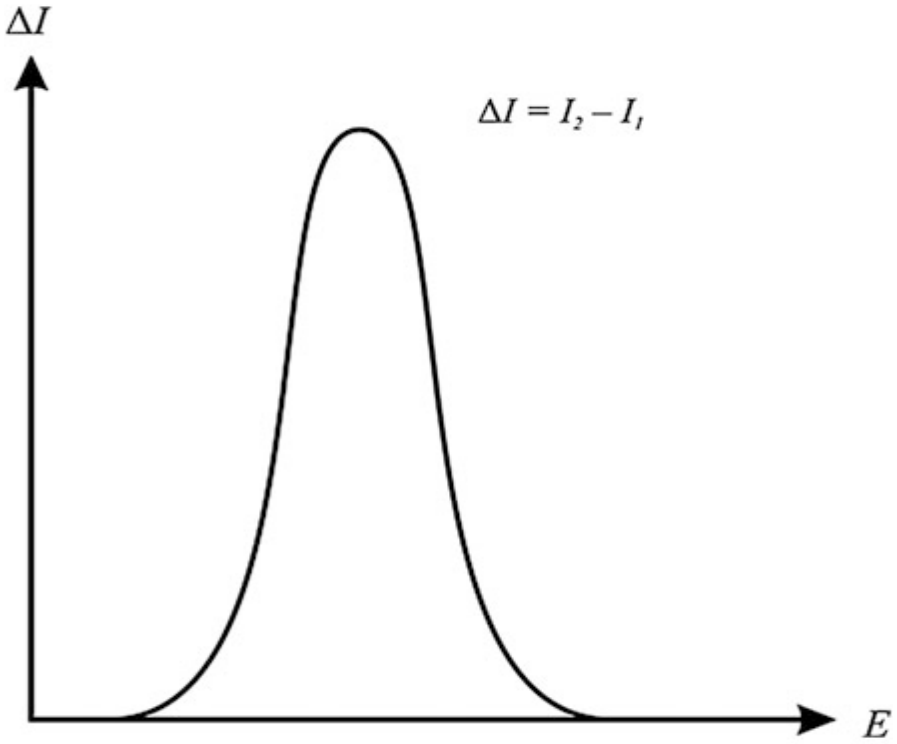

Fig 2. 10 Differential Pulse Voltammogram [67]

Summary

Ascorbic acid is an essential biomolecule found in animals and plants. It can also be found in foodstuffs like milk and soft drinks and pharmaceutical products and is used treatment of

various diseases. Conventional techniques have been used in the analysis of AA and DA with success but they present with several limits like low detection limit, high cost and tedious sample preparations. This has driven the attention into finding cheaper and sensitive techniques in the simultaneous detection since they are both detected around the same voltage potential and ascorbic acid can act as an interferent for the detection of DA.Graphene oxide and metallo-phthalocyanines have been used as electrode modifiers on their own with great success. A modifier based on the combination of graphene oxide and metallo-phthalocyanines is made to combine their effects and create a sensitive modifier for the simultaneous detection of ascorbic acid and dopamine.

CHAPTER THREE

METHODOLOGY

3.0 Introduction

The chapter introduces the materials and equipment used during the course of the research. It defines the synthetic routes used to make different compounds and the characterization techniques used. It again shows the electrochemical techniques used to analyze the analytes.

3.1 Reagents and Chemicals

Chemicals used in this study were of pure analytical grade and used directly without further purification unless stated. Potassium ferrocyanide ($K_4[Fe(CN)_6]$),potassium ferricyanide ($K_3[Fe(CN)_6]$),sodium hydroxide (NaOH), dimethyformamide (DMF) , potassium chloride (KCl) ,ethanol (C_2H_5OH),hydrochloric acid (HCl),nitric acid, nickel chloride from Associated Chemical Enterprises, sodium sulphide, potassium bromide (KBr) ,ascorbic acid ,dopamine,

potassium bromide (KBr) , trimellitic acid anhydride ($C_9H_4O_5$), ammonium chloride (NH_4Cl), urea ($CO(NH_2)_2$, nitrobenzene ($C_6H_5NO_2$), hydrochloric acid (HCl), thionyl chloride($SOCl_2$), tetrahydrofuran (THF), potassium dihydrogen phosphate (KH_2PO_4) from Skylabs, ammonium molybvdate ($(NH_4)_2MoO_4$),pentanol,sodium nitrate ($NaNO_3$), potassium permanganate ($KMnO_4$) , hydrogen peroxide (H_2O_2) from Glassworld, graphite flakes, sulphuric acid (H_2SO_4) from , from distilled water which was locally made by the MSU laboratory.

3.2 EQUIPMENT

FTIR spectra were obtained using Thermo scientific Model equipped with OMNIC software. UV-Vis spectra were obtained using a 756-model UV-Vis spectrophotometer. Sonicator model KQ-250B was used for agitation of samples. Electrochemical analyses were performed using Auto lab potentiostat PGSTAT 302N equipped with NOVA version 1.10 software and encompassed with a three electrochemical cell comprising of a glassy carbon electrode (GCE), platinum wire counter and Ag|AgCl reference electrode. A digital analytical balance (model JJ224BC) was used for weighing. The pH studies of the solutions were adjusted by a Thermoscientific Orion Star A211 pH meter.

3.3 Synthesis procedures

3.3.1 Nickel (II) tetra amino phthalocyanine

The synthesis of Nickel (II) tetra amino phthalocyanine was done in two steps. The first stage was to make nickel (II) tetra nitro phthalocyanine, followed by Nickel (II) tetra amino phthalocyanine in the second step [16].

Nickel (II) tetra nitro phthalocyanine, a mass of 10 g (0.058 moles) 4-nitrophthalonitrile and 60 ml 1-pentanol were added into a 3 neck flask equipped with a stirrer, thermometer and an

air condenser, stirred and heated to dissolve 0.53 g Ni ($CH_3COO)_2$ and 5 ml DBU (1, 8 Diazabicyclo undec-7-ene) were added and refluxed for 8 h. Afterwards the mixture was cooled, diluted with 60 ml of methanol and filtered. Purification was done by successive treatment with 100 ml of 5% HCl for 30 mins at 95 ^oC, followed by filtering. The precipitate was washed with water to neutrality. Afterwards 100 ml of 5% NaOH was added, boiled for 30 mins, cooled, filtered and washed with water.

A mass of 2 g (0.0027 moles) of finely divided tetra nitro nickel phthalocyanine and 50 mL water were added into a 3 neck flask equipped with a stirrer, thermometer and water condenser. Then the mixture is stirred for approximately 15 minutes for a good dispersion, followed by the addition of 20g (0.083 moles) $Na_2S·9H2O$ and stirred for approximately 5 h at 50 0C. The reduction reaction is followed and controlled by using thin layer chromatography on silica gel with chloroform: tetrahydrofurane 6:1 (v/v) as eluent. The mixture is filtered and the precipitate is washed with water and methanol and dried [69].

3.3.2 Graphene oxide nanosheets (GONS)

The synthesis of graphene oxide was done using the modified Hummer's method. A mass of 1 g graphite flakes and 0.5 g sodium nitrate were mixed with 23 ml of sulphuric acid and then placed in an ice bath to keep the temperature below 20 ^oC. The mixture was stirred and 3 g of potassium permanganate was added slowly and the stirring continued for 2 h at low temperatures. The temperature was raised to 35 ^oC and stirring was done for 1 h. A volume of 46 ml distilled water was added before the temperature was raised to 98 ^oC and the temperature was maintained for a further 30 mins. The contents were allowed to cool to room temperature and then stirred overnight at that temperature. A volume of 140 ml of distilled water and 10 ml 30 % hydrogen peroxide were added sequentially to quench the reaction. The resulting product

was centrifuged and washed with 5 % HCl and then distilled water several times until a pH of 7 is reached. The graphite oxide produced was dried in an oven at 60 ^{o}C for 24 h. To make graphene oxide nanosheets, the powder was dispersed in distilled water to make a concentration of 0.5 mg/ml and exfoliation was done using ultrasonication for 1 h. Centrifugation at 4000 rpm for 30 min followed, unexfoliated graphite was removed, and graphene oxide nanosheets (GONS) was dried at 60 ^{o}C [39,70].

3.3.3 Iron oxide nanoparticles

A mass of 2.015 g $FeCl_3.6H_2O$ and 1.008 g $FeCl_2.4H_2O$ were dissolved in 40 ml of deionized water. The solution is heated at 80 ^{o}C for 1 h while being stirred. Then 5ml of NH4OH (30% w/w) are added rapidly to it. The resulting suspension is vigorously stirred for another 1 h and then cooled to room temperature. The precipitated particles are washed five times with hot water and separated by magnetic decantation. These are called uncoated particles [10].

3.3.3 NiTAPc-GONs

A mass of 0.02 g of NiTAPc and 0.01 g of GONs were added to 3 ml $SOCl_2$ and 6 ml DMF and the mixture was stirred at 70 ^{o}C for 72 h. The resulting mixture was allowed to cool to room temperature and then centrifuged for 20 min at 4000 rpm and the supernatant was decanted. The NiTAPc-Fe_2O_3 solid was washed with tetrahydrofuran several times and then with ethanol to remove the tetrahydrofuran. The NiTAPc-GONs solid was dried at room temperature [9].

3.3.4 NiTAPc-Fe 2O3

A mass 0.03 g Fe_2O_3 was carboxylic acid functionalized by suspending it in a mixture of concentrated nitric and sulphuric acid in the ratio 3:1 and stirred for 2 h at 70^0 C. The f- Fe_2O_3

–COOH was oven dried at 110 ^{0}C for 12h. A mass of 0.1 g of NiTAPc and 0.01 g .The f- Fe_2O_3 –COOH were weighed and the procedure proceeded as for NiTAPc-GONs to give NiTAPc-Fe_2O_3.

3.3.5 NiTAPc-GONS-Fe $_2O_3$

A mass of 150 mg GONs and 150ml distilled water was sonicated for 2 h and then 300 mg of iron oxide was added to the GO dispersion and the mixture sonicated for 1hr under N_2 gas. Then it was stirred at 50^{o} C under nitrogen gas for 2 h then cooled to room temperature. Mixture was then centrifuged and decanted then washed with water and ethanol several times. Dry under vacuum 50^{o} C for 24 h to give GONs-Fe_2O_3 . A mass of 2 g of NiTAPc was combined with 5 mg of graphene in 25 ml of DMF with stirring and heated at 70 ºC for 96 h. After cooling the mixture was centrifuged and the resultant solid NiTAPc-NGO was washed several times with distilled water and ethanol. The product NiTAPc-GONS-Fe_2O_3 was produced and dried at room temperature [71].

3.4 Fourier Transform Infrared Spectroscopy (FTIR)

NiTAPc, GONS, Fe_2O_3 and their conjugates were characterized with FTIR using potassium bromide. The compound and potassium bromide were mixed in the ratio of 1:100 respectively. The mixture was ground to a homogenous mixture using a pestle and a motor, a small portion of the mixture was compressed to form a transparent pellet using chrome bolt and a nut. The sample was then placed into the FTIR spectrophotometer and analysed in the range 397 cm $^{-1}$ to 3897 cm $^{-1}$. The procedure was done for all the synthesized compounds NiTAPc,GONs, Iron oxide nanoparticles, NiTAPc-Fe_2O_3, NiTAPc-GONs and NiTAPc-GONs-Fe_2O_3 [37].

3.4.1 UV-Vis characterization

Iron oxide and graphene oxide were dispersed in distilled water (10 mg in 200 ml) and sonicated for 1 h. The absorbance of Fe_2O_3 was recorded at different wavelengths from the range 200-900 nm [38]. For the characterization of phthalocyanine containing compounds, DMF was used as the solvent, the concentration was 1×10^{-6} M and a scan between 300-900 nm was used.

3.5 Electrochemical characterization of electrode modifiers

Prior to use, the bare GCE was thoroughly polished with alumina slurry on a Buehler-felt pad and then washed with distilled water between each polishing step. To remove any impurities, the GCE was sonicated for 5 mins in distilled water and allowed to dry before modification. The GCE was then modified using the drop-dry method, where an aliquot of the modifier (1mg/ml in DMF) was placed on the surface of the electrode and allowed to dry in an oven at 60 ^oC. The electrodes were designated as Fe_2O_3/GCE, NiTAPc/GCE**,** NiTAPc-GONS-Fe_2O_3/GCE, NiTAPc-GONS/GCE and NiTAPc-Fe_2O_3/GCE. (See Table 3.1)

Table 3. 1: Working electrodes used in this research

Electrode modifier	Method of modification	Electrode designation
Glassy carbon electrode	-	GCE
Nickel tetra amino phthalocyanine	Drop and dry	NiTAPc/GCE
Iron oxide nanoparticles	Drop and dry	Fe_2O_3/GCE

Nickel tetra amino phthalocyanine-Fe_2O_3	Drop and dry	NiTAPc-Fe_2O_3/GCE
Nickel tetra amino phthalocyanine-GONs	Drop and dry	NiTAPc-GONs/GCE
Nickel tetra amino phthalocyanine-GONs-iron oxide nanoparticles	Drop and dry	NiTAPc-GONS-Fe_2O_3/GCE

Electrochemical characterization of electrode modifiers involves the study of the electrochemical behavior of the modified electrodes which helps to evaluate electron transfer kinetics. Evaluation of electron transfer kinetics were investigated on modified electrodes using cyclic voltammetry and electrochemical impedance spectroscopy. The characterization was performed on GCE, Fe_2O_3/GCE, NiTAPc/GCE**,** NiTAPc-Fe_2O_3/GCE, NiTAPc-GONS/GCE and NiTAPc-GONS- Fe_2O_3/GCE.

3.5.1 Cyclic voltammetry of modifiers in 1mM [Fe (CN)6] 3-/4 solution

CV, EIS and scan rates was used for the investigation of electron transfer abilities and structural differences for the bare GCE, Fe $_2$O $_3$/GCE ,NiTAPc/GCE**,** NiTAPc-Fe_2O_3/GCE, NiTAPc-GONs/GCE and NiTAPc-GONs-FE_2O_3/GCE in 1 mM [Fe (CN) 6] $^{3-/4-}$ in 0.1 M KCl at a scan rate of 100 mV/s from -0.2 to 0.6 V.

3.5.2 Electrochemical impedance Spectroscopy

Electrical impedance spectroscopy and Bode plots studies were investigated in 1 mM $[Fe(CN)_6]^{-3/-4}$ on the bare GCE, Fe_2O_3/GCE, NiTAPc/GCE**,** NiTAPc-Fe_2O_3/GCE, NiTAPc-GONs/GCE and NiTAPc-GONs-FE_2O_3/GCE in 1 mM $[Fe(CN)_6]^{3-/4-}$ in 0.1 M KCl to evaluate electron transfer resistance and structural difference of the electrodes.

3.6 optimization of pH

Optimization of pH was done in 0.1 M phosphate buffer solution whose pH was regulated using 0.1 M NaOH and 0.1 M HCl. The pH was studied in a range of 4-8 for both ascorbic acid and dopamine. Cyclic voltammetry was used for the pH optimization studies using NITAPc-GONS-Fe_2O_3/GCE and the scans were carried out from 0-0.7 V for AA and -0.4-0.8 V for dopamine using a scan rate of 0.1 V/s.

3.7 Comparative studies for ascorbic acid and dopamine

Comparative studies carried out in separate solutions 1mM AA and 1mM DA a 0.1 M phosphate buffer of the optimum pH obtained from the pH optimization studies. This was done with cyclic voltammetry using NITAPc-GONS-Fe_2O_3/GCE from 0.0 – 0.7 V for AA and -0.4-0.8 for DA using a scan rate of 0.1 V/s. Blank cyclic voltammograms were run in phosphate buffer of the optimum pH.

3.8 Simultaneous detection of ascorbic acid and dopamine

Simultaneous detection of AA and DA was carried out in a 0.1 M phosphate buffer of the optimum pH obtained from the pH optimization studies using equal concentrations of both

analytes. This was done with cyclic voltammetry using NITAPc-GONS-Fe_2O_3/GCE from 0.0 - 1 V using a scan rate of 0.1 V/s.

3.9 EIS in analytes

This was carried out in separate solutions of 1 mM AA and1mM DA in 0.1 M phosphate buffer of pH 7. This was done to analyze the behaviour of the electrodes in analyte solutions.

3.10 Kinetic studies

Scan rate studies were done using cyclic voltammetry at scan rates ranging from 30-350 mV. The electrode used was the NiTAPc-GONS-Fe_2O_3/GCE at a potential range of 0-0.8 V. A plot of anodic peak current (I_{pa}) v the square root of scan rate showed if the detection of AA and DA was diffusion controlled or not.

3.11 DPV analysis

Simultaneous detection of AA and DA was again carried out for dpv in equal concentrations of analytes. The concentrations were then varied to see the effect of the difference in concentration of one analyte has to the other. The study was also carried out in separate solutions of each analyte. The study was carried out in a 0.1 M phosphate buffer of pH 7 using a potential range of 0 – 0.8 V. The electrode used to carry out this study was NiTAPc-GONS-Fe_2O_3/GCE.

3.12 Catalytic rate constant determination

Chronoamperometry was used to determine the catalytic rate constant. The study was first done in a 0.1 M phosphate buffer of pH 7 without the analyte. Different concentrations were then

used to carry out the study for each analyte. The results were then used to deduce the catalytic rate constant. The electrode used to carry out this study was NiTAPc-GONS-Fe_2O_3/GCE.

3.13 Gibbs free energy determination

Linear sweep voltammetry was carried out to determine the Langmuir adsorption isotherm. The study was performed by using working standard solutions of AA and DA 10 μM, 20μM, 30μM, 40 μM and 50μM prepared from serial dilution of 1 mM AA and 1mM in phosphate buffer solution pH 7 .The response behavior was observed on NiTAPc-GONS-Fe_2O_3/GCE.

3.14 Interference Studies

Interference studies were done using citric acid as the interferent and DPV was used for this study. Citric acid was analyzed in a 0.1 M pH 7 phosphate buffer solution on its own to check the potential at which it is detected. Citric acid was then added to the analytes in equal concentrations and a DPV analysis was done using NiTAPc-GONs-Fe_2O_3/GCE to check if its presents can affect the detection of AA and DA.

3.15 Reproducibility studies

The reproducibility study of the chemical sensor was investigated through repetitive measurements of 100 μM AA and 100 μM DA in 0.1 M pH 7 phosphate buffer solution by differential pulse voltammetry from 0.0 to 0.8 V. After each run, the electrode was washed with ethanol and the procedure was repeated four times.

3.16 Stability Studies

For stability studies, cyclic voltammetry was used, 20 continuous cycles were run in 1 mM AA and 1 mM DA in 0.1 M phosphate buffer (pH 7) using a scan rate of 0.1 V/s.

Summary

This chapter highlights the experimental part of the research. Different chemical modifiers were synthesized and characterized using physical and electrochemical techniques. The modifiers were used in the simultaneous detection of ascorbic acid and dopamine to see the best electrode that can used for further studies.

CHAPTER FOUR

RESULTS AND DISCUSSION

4.0 Introduction

The chapter highlights all the results and findings obtained from various experiments done in this research. The results obtained are further discussed in detail and compared to work published by other researchers.

4.1 Synthesis of electrode modifiers

Different electrode modifiers were synthesized for the detection of ascorbic acid and dopamine which are Fe_2O_3, NiTAPc, GONs, NiTAPc-GONS, NITAPc-Fe_2O_3 and NITAPc-GONS-Fe_2O_3.To ensure that Fe_2O_3 was successfully synthesised its magnetic property was tested. A magnetic stirrer was placed in aqueous solution of the iron oxide nanoparticles. Fe_2O_3 were attracted to the magnetic stirrer. This confirmed its magnetic properties reported in other works [8].

NiTAPc that was synthesised had a green colour which is characteristic colour or most amino phthalocyanines. NiTAPc was synthesised as below with Me being the metal centre Ni from Ni $(CH_3COO)_2$.

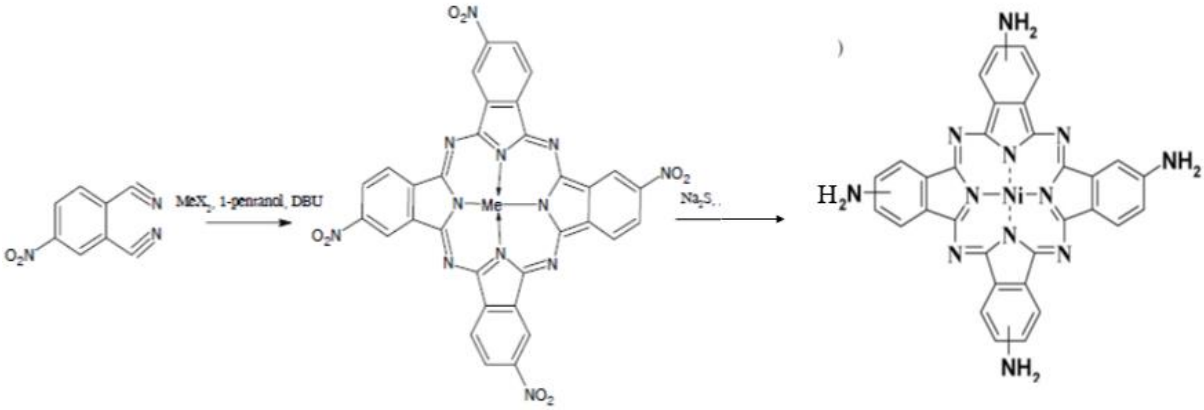

When synthesizing GONs-NiTAPc, thionyl chloride was used to activate the carboxylic functional groups of GO by converting the carboxylic group (-COOH) groups to acyl groups (-COCl). The acyl groups then readily react with the amine groups ($-NH_2$) of NiTAPc forming covalent linkages by amide bonds formation (O=C-NH).

4.2 Characterization of electrode modifiers

4.2.1 Fourier Transfer Infrared Spectroscopy (FTIR)

The synthesized electrode modifiers were characterized by FTIR within the range of 400-4000 cm^{-1}. Figure 4.1 shows the stacked FT-IR spectra of GONS, Fe_2O_3, NiTAPc, NiTAPc-GONS, NITAPc-Fe_2O_3 and NITAPc-GONS-Fe_2O_3.

The FTIR of GONS showed the presence of a peak at 1150cm-1 which is attributed to the C-O bond, confirming the presence of oxide functional groups after the oxidation process. The peak at 1631 cm-1 shows the presence C=C bond which still remained before and after the

oxidation process. The absorbed water in GO is shown by a broad peak at 3322 cm-1 to 3652 cm-1, contributed by the O-H stretch of H_2O molecules. This supports the fact that GO is a highly absorptive material, as verified by its ability to become a gel-like solution. The FTIR spectrum for the Fe $_2$O $_3$ shows main bands at 3442 cm-1 for the O-H stretching, 1635 cm-1 O-H bending and 590 cm-1 Fe-O stretching. The analysis of the IR spectra of the NiTAPc shows the presence of the bands characteristic to the primary aromatic amines with stretching of the N-H bond at 3451 cm-1 and the in plane deformations of the N-H bond at 1645 cm-1. The other characteristic bands of the aromatic amino group, namely the stretching vibrations of the C-N bond is found at peak 1249-1346 cm-1 and the out plane deformation vibrations of the N-H bond found at 625-900 cm-1 are overlapping with the characteristic bands of the phthalocyanines. On the spectra for NiTAPc-GONs an amide peak at around 1618cm−1 (in-between the –NH2 vibration mode and the C O stretching peak) is a clear indication of coordination between NiTAPc and GONs.An amide peak at around 1630 for NITAPc-Fe_2O_3 shows the covalent linkage between NiTAPc and Fe_2O_3.

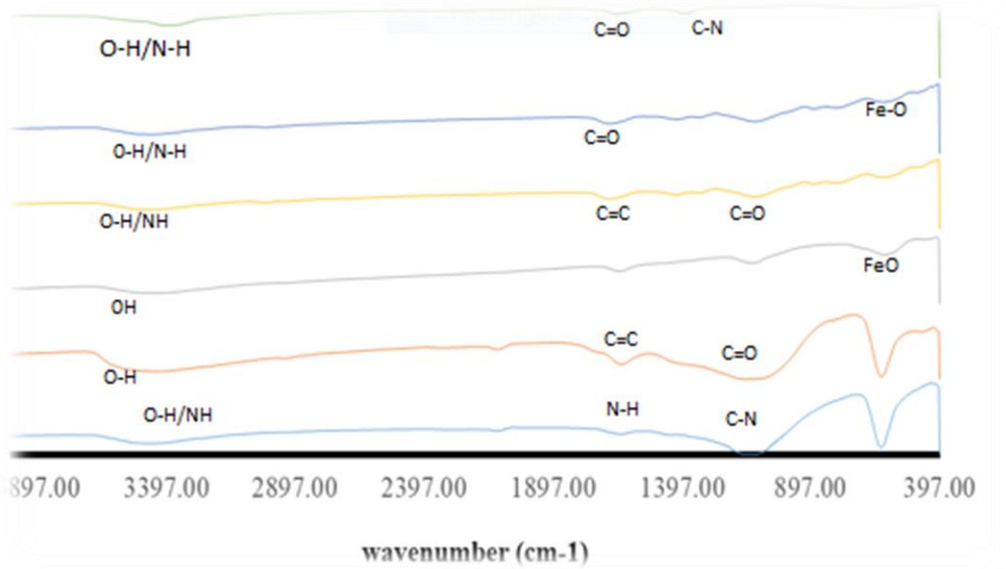

Fig 4. 1 FTIR spectrum of synthesized electrode modifiers

4.2.2 Ultraviolet Visible Spectroscopy

Phthalocyanines are known to show two strong adsorption peaks in the regions 300-400 nm and 600-700 nm. A peak in the first region of 300-400 is known as the Soret band and a peak in the region of 600-700 nm is known as the Q band. From the UV-vis spectra of NiTAPc (a) the Soret band was observed and it is a result of deeper π levels of LUMO transitions. The Q band was also observed and it is attributed to the π-π* electron transition from the HOMO to the LUMO of the phthalocyanine ring. The spectrum of the modifier NiTAPc-GONS (b) showed the red shifting of the Soret band and the Q band which is again attributed to the successful combination of the two. Upon modification of the NiTAPc with GONs, there is a substantial increase in the absorbance of the B-band of NiTAPc at 310 nm due to the overlap of the GONs with the NiTAPc. NiTAPc-Fe $_2O_3$ (c) showed a shift of the Q band to a wavelength of 685nm from 705nm. NITAPc-GONs-Fe_2O_3 (d) showed a shift on the Q band from to a wavelength and an increase in the absorbance at the B band due to the overlap of the GONS, iron oxide and NiTAPc. The spectrum for iron oxide (a) showed a characteristic absorption peak at 400nm and GONs (b) showed an expected absorption peak at 260nm.

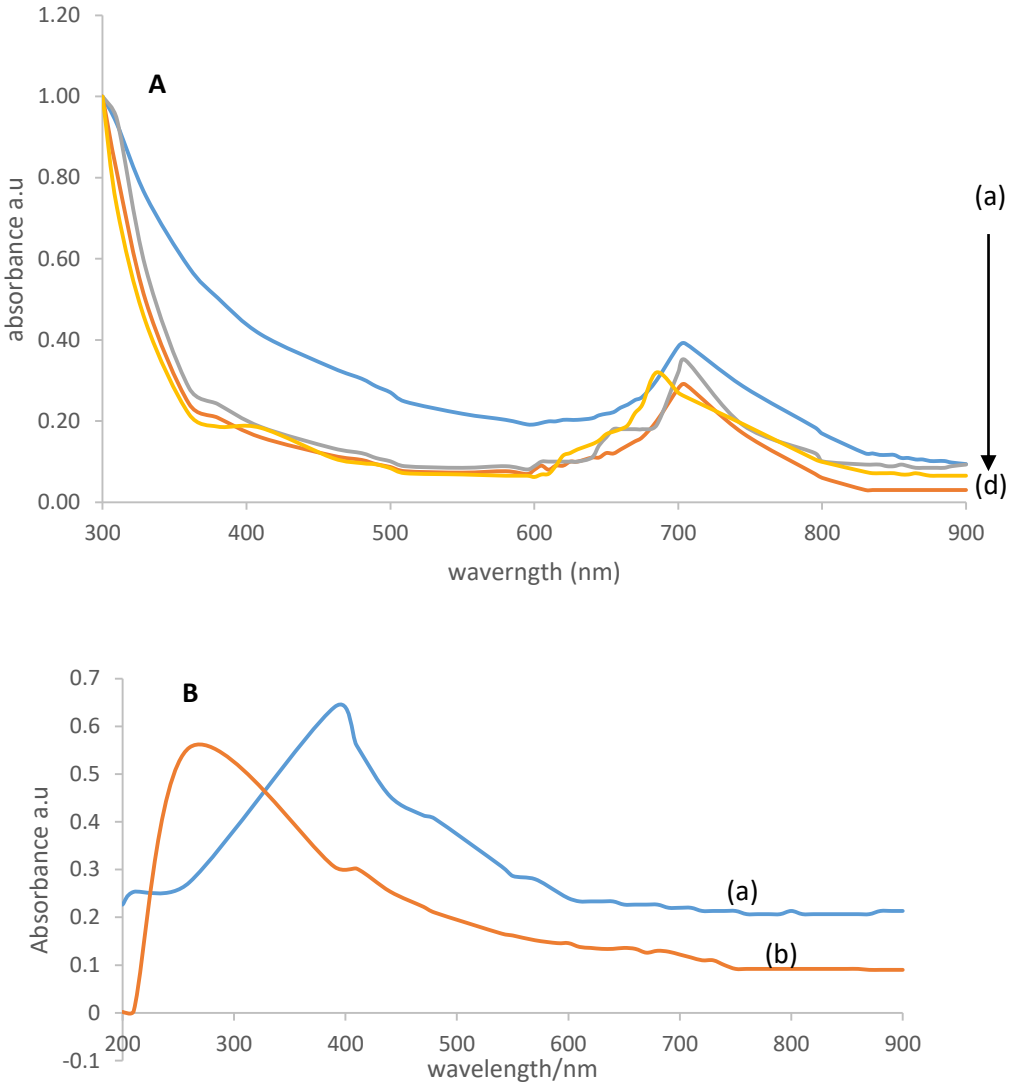

Fig 4. 2 (A) and (B) UV-vis spectrum of electrode modifiers

4.3 Electrochemical Characterization

4.3.1 Cyclic Voltammetry

Electrochemical behaviour of redox probe in 1 M KCl was investigated at bare-GCE, Fe_3O_4 NPs -GCE, NiTAPc-GCE, NiTAPc-GONS-GCE, NiTAPc-Fe_2O_3NPs-GCE and NiTAPc-GONS-Fe_2O_3NP-GCE CVs are depicted in Fig 4.3.

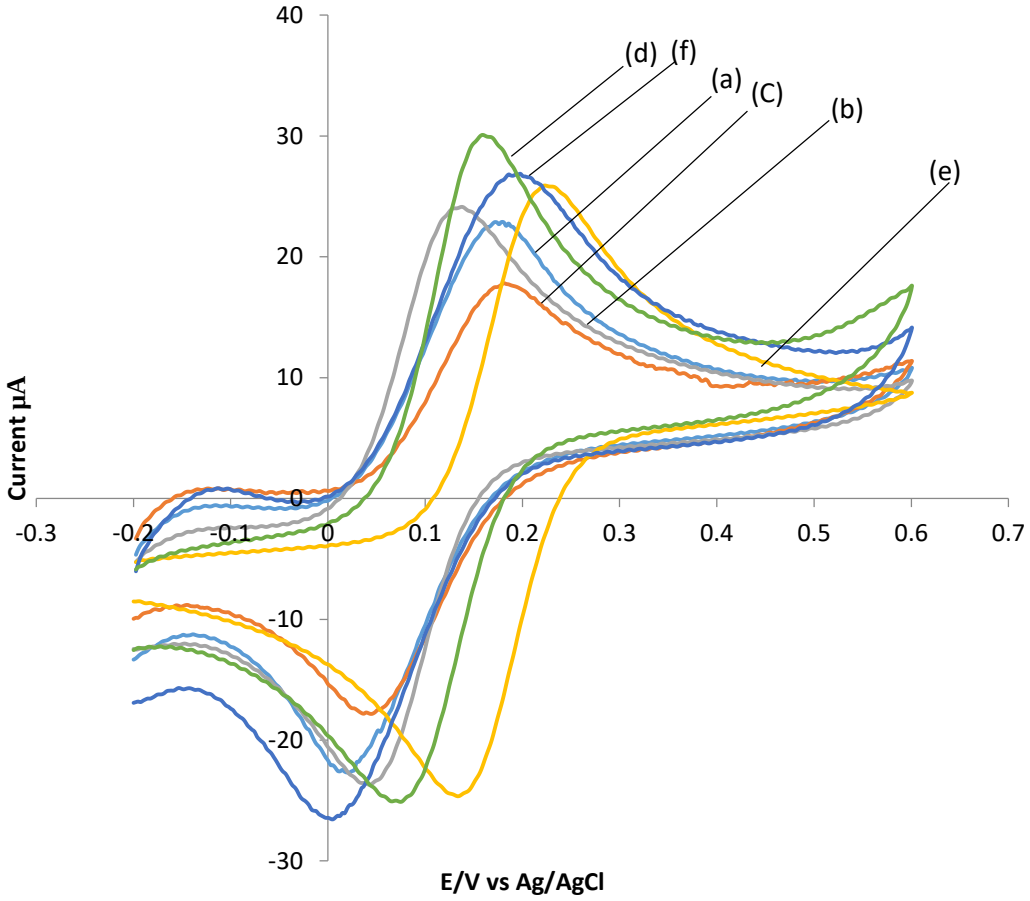

Fig 4. 3: Voltammograms of GCE (a), Fe_3O_4NPs -GCE (b), NiTAPc-GCE (c), NiTAPc-GONs-Fe_2O_3NP -GCE (d) ,NiTAPc-Fe_2O_3NPs-GCE (e) and NiTAPc-GONs-GCE (f) Bare-GCE in equimolar solution of 1mM $K_3[Fe(CN)_6]^{3/4-}$ prepared in 1 M of KCl. Scan rate = 100 mV/s

A well-defined pair of redox peaks attributable to one electron transfer $Fe(CN)_6^{3-/-4}$ of are seen in all cases. Comparatively the peak-to-peak separation , ΔEp for $Fe(CN)_6^{3-/-4}$ redox

couple was observed to be 85 mV at GCE, 132 mV Fe_3O_4 NPs -GCE, 144 mV NiTAPc-GCE, 112 mV NiTAPc-Fe_3O_3-GCE, 82 mV NiTAPc-GONs-GCE and 78 mV NiTAPc-GONs-Fe_2O_3–GCE (Table 4.1). The order in terms of electron transfer efficiency is therefore NiTAPc-GONs-Fe_2O_3–GCE (78 mV) > NiTAPc-GONs-GCE (82 mV) > Bare-GCE (85 mV) >

NiTAPc-Fe_3O_3NPs -GCE (112 mV) > Fe_3O_4 NPs -GCE (132 mV) > NiTAPc-GCE (144 mV). The higher peak currents and smaller ΔEp values in cyclic voltammetry recorded for 1mM $K_3[Fe(CN)_6]$ redox probe in 1mM KCl over NiTAPc-GONs-Fe_2O_3-GCE suggest the facilitation of electron transfer for $Fe(CN)_6^{3-/-4}$ redox couple due to the synergistic effect of NiTAPc , GONs and Fe_2O_3 ions present in the composite. The electron transfer kinetics of the modifiers on the surface of glassy carbon electrode were also confirmed by the increase in anodic peak current. The order of electron transfer is therefore GCE > NiTAPc-GCE > Fe_2O_3 -GCE > NiTAPc-Fe_3O_3 -GCE > NiTAPc-GONs-GCE > NiTAPc-GONs-Fe_2O_3–NPs-GCE.

The smaller Ep (78 mV)and high Ipa (31.29µA) value for NiTAPc-GONS-Fe_2O_3–GCE is indicative of decoration of iron oxide nanoparticles on the surface of graphene oxide nanosheets conjugated nickel tetra amine phthalocyanines hence improving electron transfer properties of the composite [5] .

The surface roughness factor of the modified electrodes were determined using was $[Fe(CN)_6]^{3-/4-}$ redox system and applying the Randles –Sevcik Equation for reversible system [39][55].

$$I_p = (2.69 \times 10^5)n^{3/2}D^{1/2}CAv^{1/2} \qquad (4.0)$$

Where Ip the peak current, n is equal to the number of electrons transferred at the surface of the electrode, D is the diffusion coefficient of the analyte in solution 7.6 x 10^{-6} cm^2/s^{-1} and C

is the solution concentration in (mol/cm^{-3}),A is the effective surface area and v is the scan rate (V/s^{-1}).

The surface roughness factors (ratio of Ipa experimental /Ipa theoretical) were determined for all the probes and the corresponding real electrode areas (roughness factor x theoretical surface area (=0.208cm^2) were determined. The real electrode area for NiTAPc-GONs-Fe_2O_3 -GCE is larger than the bare electrode 0.071 cm^2.Therefore the NiTAPc-GONs-Fe_2O_3 -GCE is expected to perform better than all electrodes based on the effective electrode area. Table 4.1 below gives summary parameters.

4.3.2 Electrochemical Impedance Spectroscopy (EIS) Characterization

Electrochemical impedance spectroscopy (EIS) is a potent tool for the proper determination of both kinetic and mass-transport parameters as well as the charge transfer coefficient. Fig 4.4 shows the EIS response for GCE, Fe $_2O_3$-GCE, NiTAPc-GCE, NiTAPc-GONs-GCE, NiTAPc-Fe_2O_3-GCE and NiTAPc-GONS-Fe_2O_3-GCE .The curve of the EIS includes a semi-circular part and a linear part. The semi-circular diameter is equivalent to the electron transfer resistance which controls the electron transfer kinetics of the redox probe at the electrode interface.

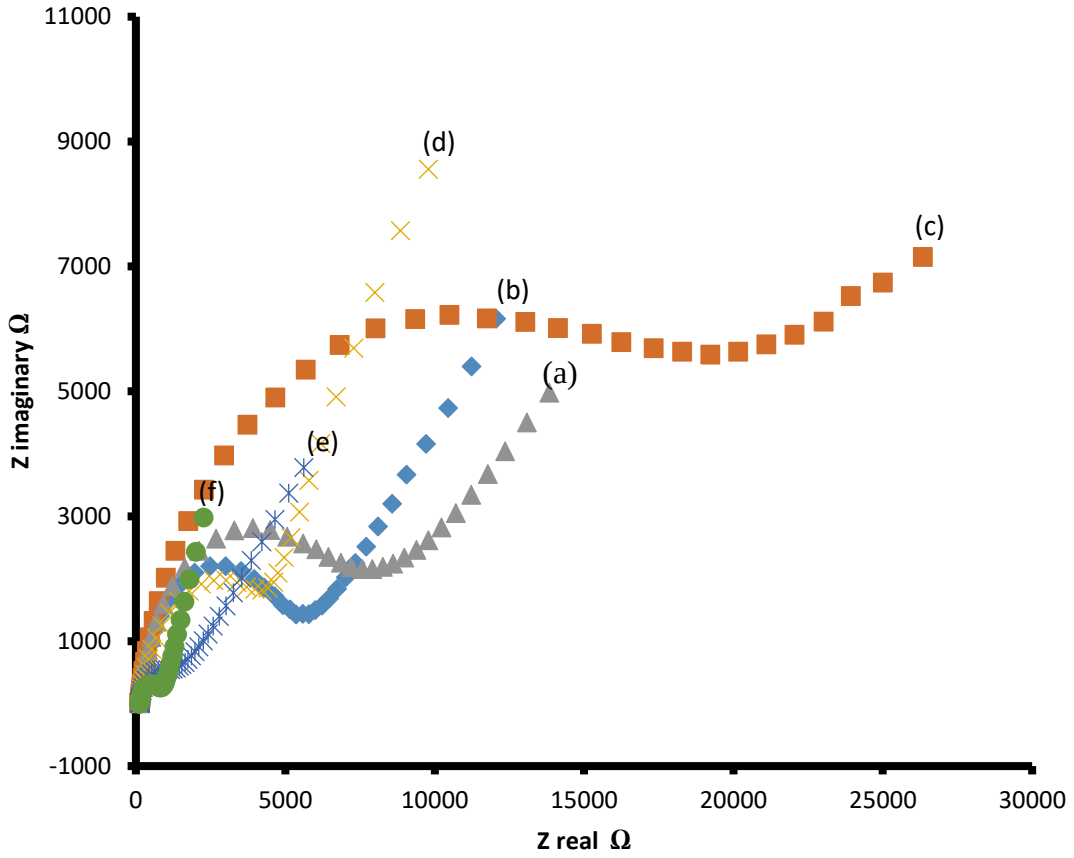

Fig 4. 4 Nyquist plots obtained of bare (a) ,Fe_3O_4NPs -GCE (b), NiTAPc-GCE (c), NiTAPc-GONS –GCE (d), NiTAPc-Fe_2O_3NPs-GCE (e) and NiTAPc-GONS-Fe_2O_3NP-GCE (f) in equimolar solution of 1mM $[Fe(CN)_6]^{3-/4-}$ prepared in 1 M of KCl. Scan rate = 100 mV/s

The semicircle equals to the electron transfer resistance (R_{CT}) which decreases with the improvement of electron transfer. As shown in Fig 4.4 the R_{CT} of NiTAPc-GONs-Fe_2O_3NP-GCE is the smallest during the redox process implying good conductivity. Upon modification of GCE by Fe_2O_3 , the R_{CT} increased from 4.92 kΩ (GCE) to 7.92 kΩ indicating that the electron transfer from the redox probe of $[Fe(CN)_6]^{3-/4-}$ to the electrode surface was hindered. The high resistance might have been caused by the aggregation of Fe_2O_3 could diminish the electron transfer process [9]. The high R_{CT} value of NiTAPc indicates that on its own NiTAPc has a small electron transfer property. Moreover the decoration of Fe_2O_3 nanoparticles on

NiTAPc significantly increased surface area and enhanced the electrical conductivity of the electrode accounting for the decrease of R_{CT} as compared to the individual electrodes .The R_{ct} reduced from 1.16 kΩ (NiTAPc-Fe_2O_3NPs) to 0.86 kΩ (NiTAPc-GONS-Fe_2O_3NPs) as graphene oxide nanosheets were conjugated with NiTAPc and Fe_2O_3 hence their synergistic effect resulted in the decrease of R_{ct} value indicating the incorporation of a catalytic material within the composite. Generally the electron transfer efficiency of the modified electrode has been enhanced after the introduction of graphene nanosheets and Fe_2O_3 nanoparticles into the NiTAPc.

The order of decrease of electron transfer efficiency (in the form of decrease in Rct) is as follows: NiTAPc-GONS-Fe_2O_3–GCE > NiTAPc-GONS -GCE) > Bare-GCE > NiTAPc-Fe_3O_3NPs -GCE > Fe_3O_4 NPs -GCE > NiTAPc-GCE. EIS results are in agreement with CV measurements demonstrating the successful fabrication of the sensor.

The R_{ct} can be used to calculate the heterogeneous electron transfer rate constant (kapp) across the electrode interface under study. The R_{ct} is inversely proportional to (kapp) constant, in according to the Equation:

$$kapp = RT/FRctC$$

Where C is the concentration ($[Fe(CN)_6]^{3-/4-}$1.0 x 10^{-3} mol cm^{-3}), with R and F having their usual meanings. The decrease in k_{app} value (Table 4.1) from NiTAPc-GONS-Fe_2O_3–GCE (2.98 x 10^{-2} cm s^{-1}) > > NiTAPc-GONS -GCE (2.21 x 10^{-2} cm s^{-1}) > NiTAPc-Fe_3O_3NPs -GCE (5.63 x 10^{-3} cm s^{-1}) > Fe_3O_4 NPs -GCE (3.35 x 10^{-3} cm s^{-1})> NiTAPc-GCE (1.33 x 10^{-3} cm s^{-1}) ,indicating that electron transfer process between the redox and the underlying bare surface are much easier at NiTAPc-GONs-Fe_2O_3–GCE compared to other electrodes [57] . The higher k_{app} value obtained for the $[Fe(CN)_6]^{3-/4-}$ redox at NiTAPc-GONs-Fe_2O_3–GCE in comparison to other electrode systems indicates that the presence of Fe_2O_3 nanoparticles and the formation of

an amide linkage between NiTAPc and graphene nanosheets hence facilitating the electron transfer reaction to higher extent as compared to other individual electrodes.

Table 4. 1 Electrochemical parameters for the modified electrodes

ELECTRODE	$\boldsymbol{\Delta E_{(pa-pc)}(mV)}$	A_{EFF}	K_{APP}/CMS^{-1}	$R_{CT}(K\Omega)$
GCE	85	-	1.25×10^{-2}	4.92
NITAPC-GCE	144	0.147	5.63×10^{-3}	8.24
FE_2O_3-GCE	132	0.158	3.35×10^{-3}	7.92
NITAPC-GONS –GCE	82	0.181	2.27×10^{-2}	0.86
NITAPC-FE_2O_3–GCE	112	0.164	5.63×10^{-3}	1.16
NITAPC-GONS-FE_2O_3–GCE	78	0.208	2.98×10^{-2}	0.41

Bode plots

Bode plots (Fig 4.5) were used to obtain frequency related information which is a plot of phase-shift vs. log frequency, which cannot be obtained from their Nyquist plots. The nature of the Bode plots confirmed the structural differences of the GCE modified electrodes and the GCE. After modification of the glassy carbon electrode with NiTAPc, GONs, $Fe_2 O_3$ and peaks shifted to lower frequencies indicating that electrocatalysis is occurring at the surface of the modified glassy carbon electrode. Phase angles were decreasing and they were less than the ideal 90^0 for an ideal capacitor [61]. Surfaces with the phase angle shifted towards lower frequencies in the Bode plot indicate better catalytic efficiency. Changes in phase angles and frequencies is an indication of the structural differences of the surfaces, and that more oxidation

of the analyte is likely to occur at the modified surfaces rather than on the bare GCE.

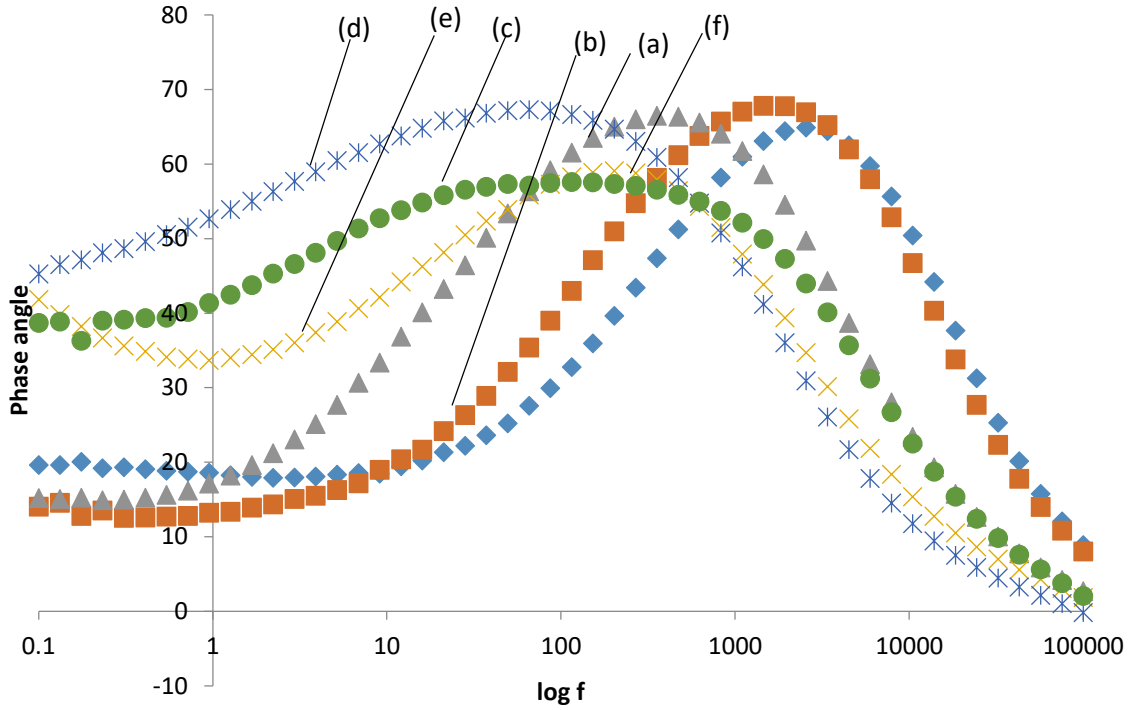

Fig 4. 5 Bode Plots obtained for bare (a), Fe_3O_4NPs -GCE (b), NiTAPc-GCE (c), NiTAPc-GONS –GCE (d), NiTAPc-Fe_2O_3NPs-GCE (e) and NiTAPc-GONS-Fe_2O_3NP-GCE (f) in equimolar solution of 1mM $[Fe(CN)_6]^{3-/4-}$ prepared in 1 M of KCl. Scan rate = 100 mV/s

4.4 Electro catalytic detection of dopamine and ascorbic Acid

4.4.1 Effect of pH

The oxidation of 1 mM dopamine and ascorbic acid was significantly influenced by the pH of the supporting electrolyte. The variation in peak current and peak potential of ascorbic and dopamine at NiTAPc-GONs-Fe_2O_3 under the influence of change in pH was investigated in the pH range of 4 to 8 Figure 3(A and B). The oxidation peak current increases as the pH increases from 4 to 7 and decreases up to 8 .The oxidation of ascorbic and dopamine is more favourable at pH 7 and hence we have chosen pH 7 as optimum pH for all the electrochemical

studies performed in this work. This pH has also been used in previous works to detect dopamine and ascorbic acid [4].

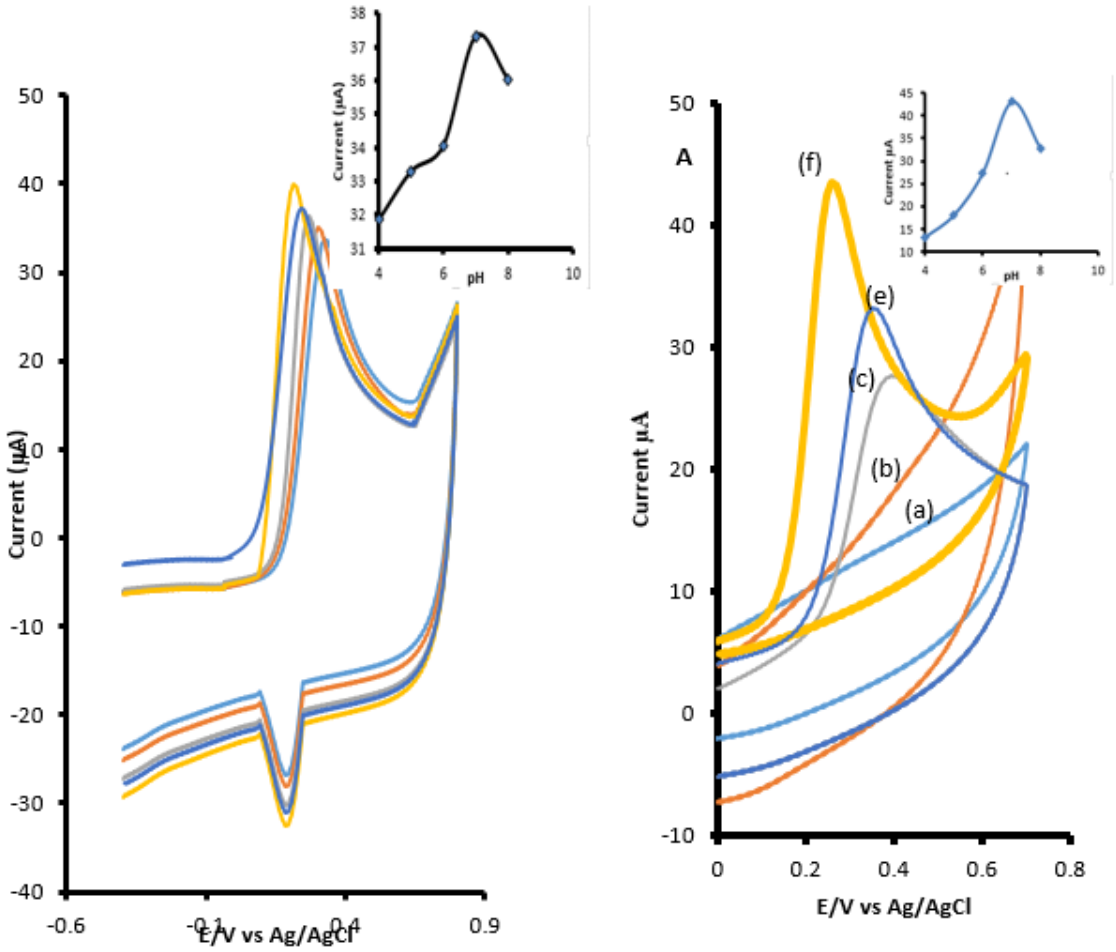

Fig 4. 6 (A and B) Cyclic voltammograms of peak currents and peak potentials (A) Dopamine (B)ascorbic acid for NiTAPc-GONS-Fe_2O_3-GCE in (a) pH 4, (b) pH 5, (c) pH 6, (d) pH 7 and (e) pH 8 phosphate buffer solution containing 1mM ascorbic acid and dopamine. Scan rate = 100 mV/s

4.5 Catalytic oxidation of Ascorbic acid

Figure 4.7 displayed the cyclic voltammograms of 1 mM AA in pH 7 PBS .As shown in Fig 4.7 oxidation peak current increased according to the following sequence of electrode modification on the electrode GCE-Fe_2O_3-GCE < NiTAPc-GCE < NiTAPc-Fe_2O_3-GCE <

NiTAPc-GONS-GCE <NiTAPc-GONS-Fe_2O_3-GCE. In the presence of 1 Mm AA NiTAPc-GONS-Fe_2O_3-GCE (f), NiTAPc-GONS-GCE (e), d) NiTAPc-Fe_2O_3-GCE , (c) NiTAPc-GCE, Fe_2O_3NPs -GCE b) provides a clear oxidation peaks at 0.256 V, 0.258 V, 0.315 V,0.356 V and 0.383 V, for ascorbic acid respectively . The GCE showed limited current and high oxidation potentials towards the detection of ascorbic acid implying insensitive electrochemical activity for the oxidation of ascorbic acid. On the contrary a typical response current of NiTAPc-GONS-Fe_2O_3-GCE appeared responding to ascorbic acid implying the NiTAPc-GONS-Fe_2O_3-GCE exhibited excellent electrocatalytic activity for ascorbic oxidation. The oxidation peak current (Ipa) of NiTAPc-GONS-Fe_2O_3-GCE was attributed to the synergetic effect of GONS, NiTAPc and Fe_2O_3 resulting in facilitating a remarkable high electron transfer indicating a more notable sensitivity toward the detection of ascorbic acid. The significant catalytic property of NiTAPc-GONS-Fe_2O_3-GCE may be attributed to numerous active sites provided by GONS and the high electron transfer properties of NiTAPc and Fe_2O_3 [51].

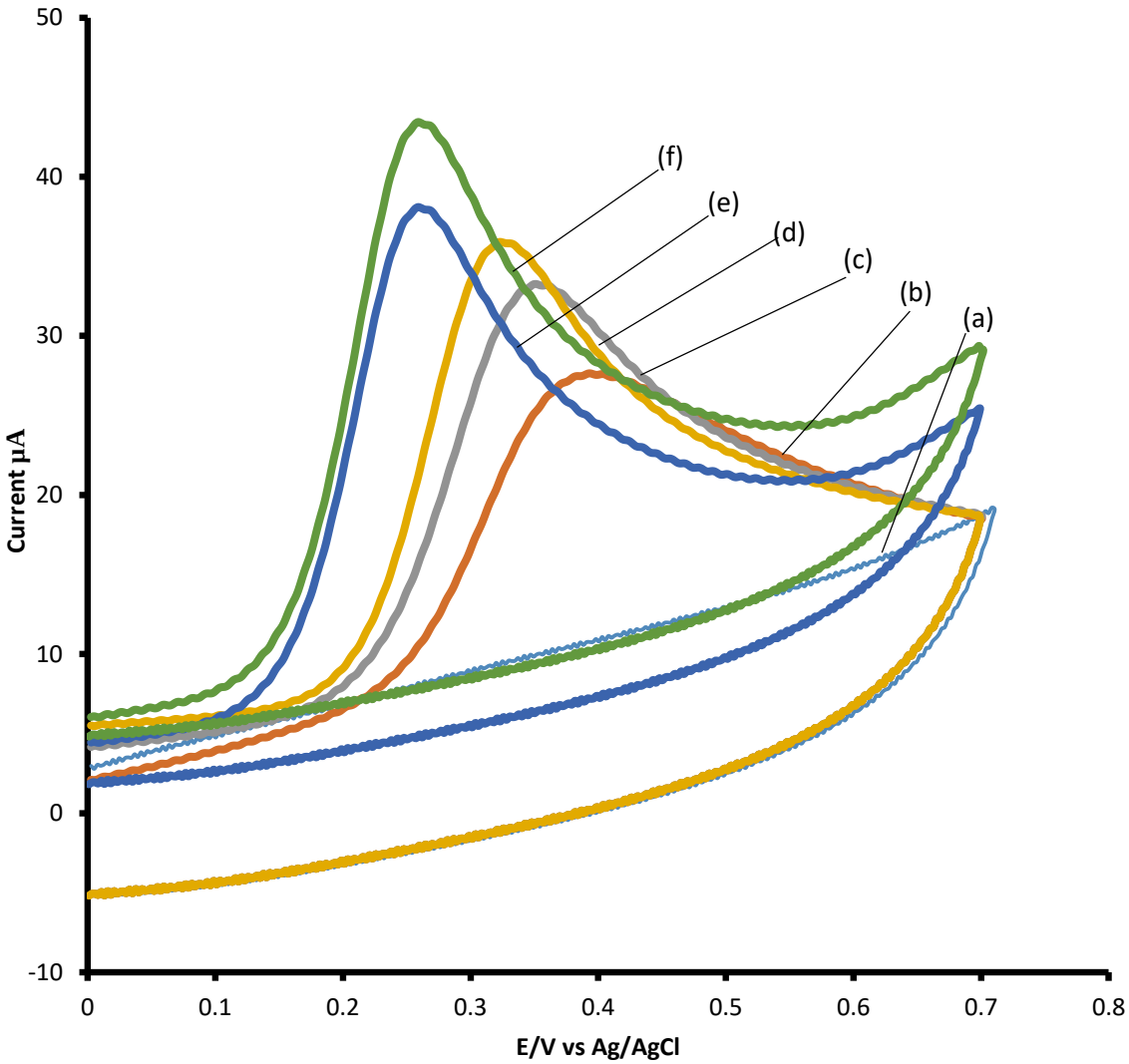

Fig 4. 7 : Voltammograms of bare (a), Fe_3O_4NPs -GCE (b), NiTAPc-GCE (c), NiTAPc-GONs -GCE (d) NiTAPc-Fe_2O_3NPs-GCE (e) and NiTAPc-GONs-Fe_2O_3NP-GCE (f) in 1mM Ascorbic acid in a 0.1 M PBS (pH 7.0) at a scan rate of 0.1 V/s.

4.6 Catalytic oxidation of Dopamine

Figure 4.8 displayed the cyclic voltammograms of 1 mM DA in pH 7 PBS at GCE and modified electrodes. The CV data indicate a quasi-reversible electro oxidation of DA. As shown in Fig

4.8 oxidation peak current increased according to the following sequence of electrode modification on the electrode GCE < Fe_2O_3-GCE < NiTAPc-GCE < NiTAPc-Fe_2O_3-GCE < NiTAPc-GONs-GCE <NiTAPc-GONs-Fe_2O_3-GCE. In the presence of 1 mM dopamine the NiTAPc-GONs-Fe_2O_3-GCE (e), NiTAPc-GONs-GCE (d), c) NiTAPc/Fe_2O_3NPs -GCE , (b) NiTAPc-GCE and Fe_2O_3NPs /GCE a) provides a clear oxidation peaks at 0.216 V, 0.243 V, 0.267 V ,0.304 V and 0.362 V for dopamine respectively . At the GCE shows limited current and no oxidation peaks observed towards the detection of dopamine implying insensitive electrochemical activity for the oxidation of dopamine. Whereas the NiTAPc-GONs-Fe_2O_3-GCE shows a significantly enhanced peak current and a more reversible electron transfer process for DA under similar conditions. A well-defined redox wave of DA was observed with respective anodic and cathodic peak potentials at 216 and 177 mV. Intensive increase witnessed in peak current could be owed to the improvement in reversibility of electron transfer process and the larger real surface area of the NiTAPc-GONs-Fe_2O_3-GCE. It is believed that the existence of graphene is an ideal support material and acts as an effective electron promoter for electrocatalytic oxidation of DA. Good synergistic effects emerged between Fe $_2O_3$ nanoparticles and graphene sheets enhance the conductive area and electron transfer rate between DA and electrode surface [3]. Aside the fact that Fe is in its most stable oxidation state of +3 in the electrolyte, which makes it a strong catalyst and oxidant, it has also been reported that Fe^{3+} is chelated by the dihydroxy catechol group of dopamine, catechol, 5, 6-dihydroxyindole . A report demonstrated that 7(2-aminoethyl)-3, 4-dihydro-5-hydroxy-2H-1,4-benzothiazine-3

carboxylic acid (DHBT-1), containing –OH phenolic and >NH in six ring, had an ability of binding Fe $^{3+}$ like 5, 6-dihydroxyindole [16]. It can therefore be concluded from these previous reports that the NiTAPc-GONs-Fe_2O_3-GCE modified electrode could be the best electrode towards DA oxidation based on the ability of Fe^{3+} to bind and form chelate with DA [14] and

its oxidation intermediates. To ensure whether the redox peak that appeared was for modifier or due to the presence of DA a blank cyclic voltammograms was recorded only for phosphate buffer Fig 4.9. Consequently, there were no peaks obtained for the modifiers, which suggests the redox peaks obtained were due to the redox behaviour of DA.

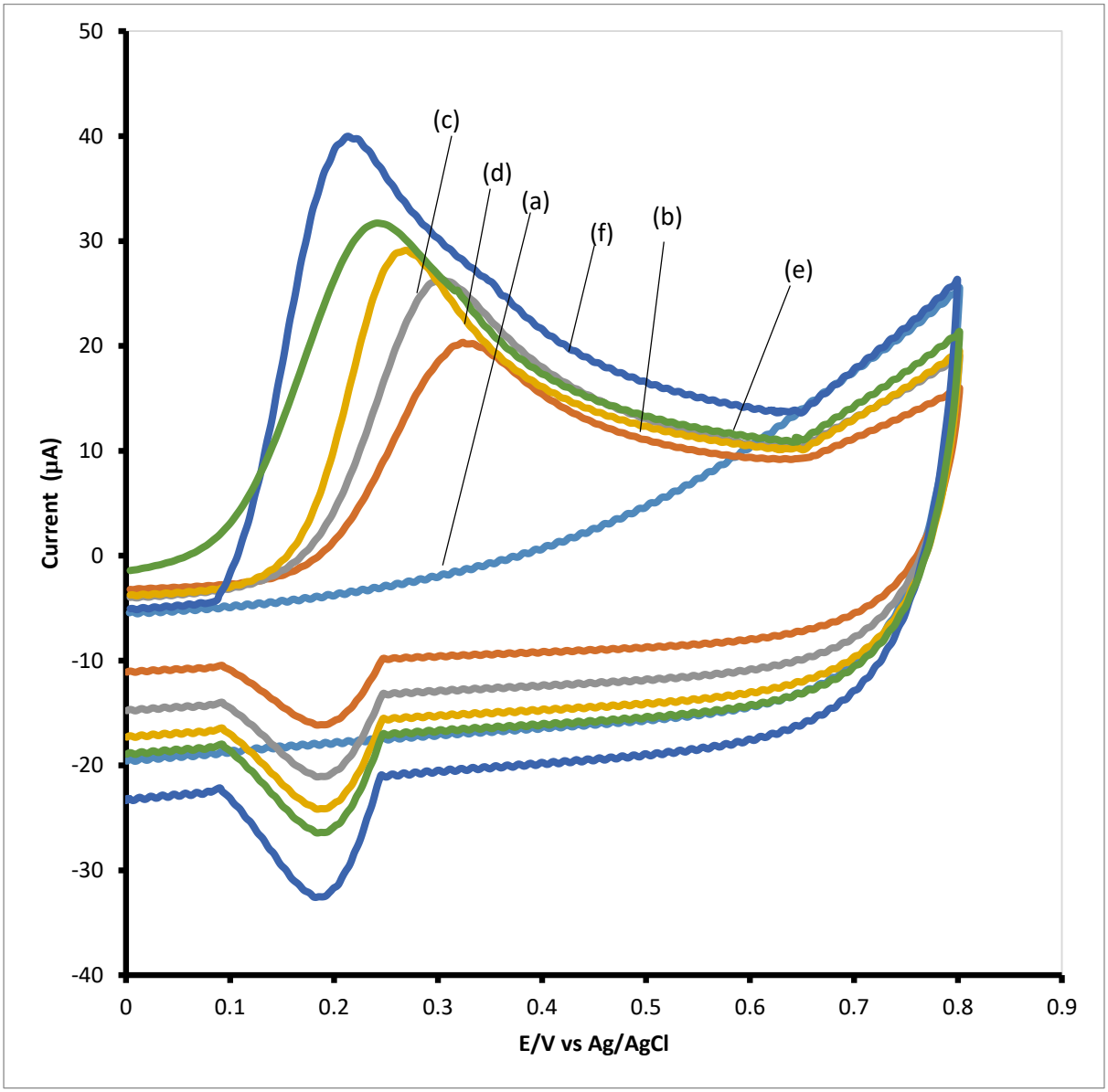

Fig 4. 8: Voltammograms of bare (a) Fe_2O_3NPs -GCE (b), NiTAPc-GCE (c), NiTAPc-Fe_2O_3 NPs -GCE (d),NiTAPc-GONS-GCE e) and NiTAPc-GONS-Fe_2O_3NPs in 1mM Dopamine in a 0.1 M PBS (pH 7.0) at a scan rate of 0.1 V/s.

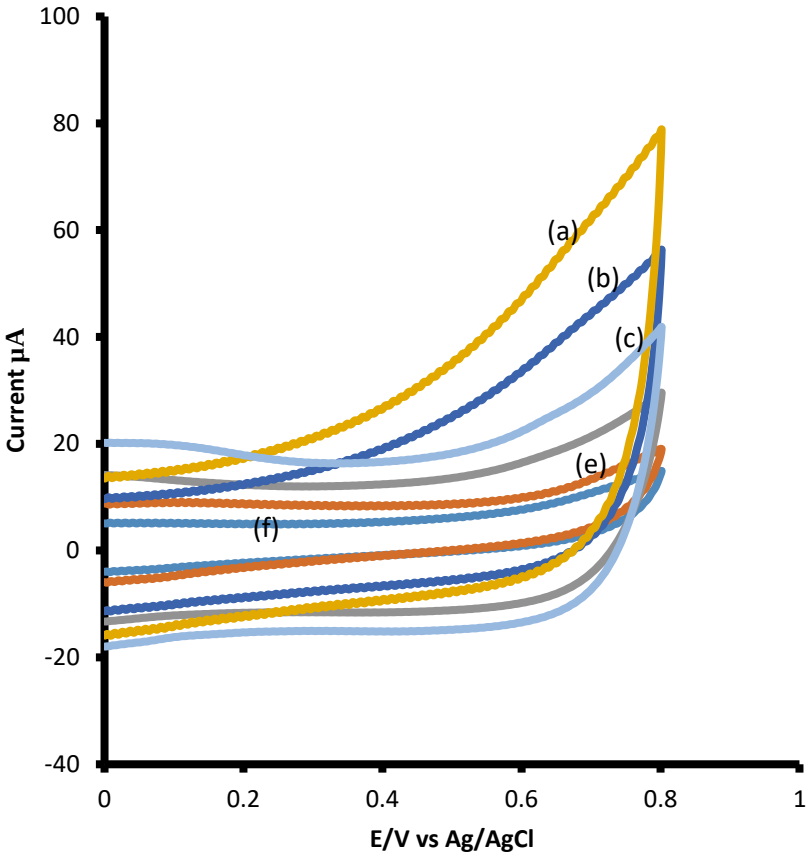

Fig 4. 9 : Voltammograms of bare (a) Fe_2O_3NPs -GCE (b), NiTAPc-GCE (c), NiTAPc-Fe_2O_3 NPs -GCE (d),NiTAPc-GONS-GCE e) and NiTAPc-GONS-Fe_2O_3NPs f) in a 0.1 M PBS (pH 7.0) blank solution at a scan rate of 0.1 V/s.

4.4 Electrochemical impedance spectroscopy

Fig. 4.10 (A and B) displays the impedance spectra of different electrodes in dopamine and ascorbic acid respectively. A Randels equivalent circuit was used in the EIS spectra to obtain value of charge transfer resistance, where the *R*s, *R*ct, *W* and QCPE refer to the solution resistance, charge transfer resistance, Warburg impedance and constant phase element .The bare GCE shows an obvious semicircle, implying the characteristic of an electron transfer limited process. After modifying the bare electrode with NiTAPc in the electrode, an obvious decrease in semicircle interfacial R_{ct} is obtained. The R_{ct} of the NiTAPc-GONs is much smaller

than those of NiTAPc-Fe_2O_3 and NiTAPc-GCE, suggesting that NiTAPc-GONs could serve as a good electron-transfer interface between the electrode and the analytes. It has been reported that the straight line observed suggests that graphene sheets can facilitate the electron transfer process. However, coupling the magnetic particles with graphene sheets, the EIS of modified electrodes display almost a straight line, indicating low interfacial electron transfer resistance and promotion of electron transfer process for the nanocomposites. This may be attributed to the larger surface area and good conductivity of the GONs and Fe_2O_3 nanocomposites [20]. When the NiTAPc-GONs-Fe_2O_3 composite was introduced on GCE, we observe that the diameter decreases further, indicating that the NiTAPc-GONs-Fe_2O_3NPs could more effectively accelerate the electron-transfer, which is ascribed to the synergistic effect of NiTAPc, GONs and Fe_2O_3. The lesser resistance by modified electrode towards the charge transfer processes.

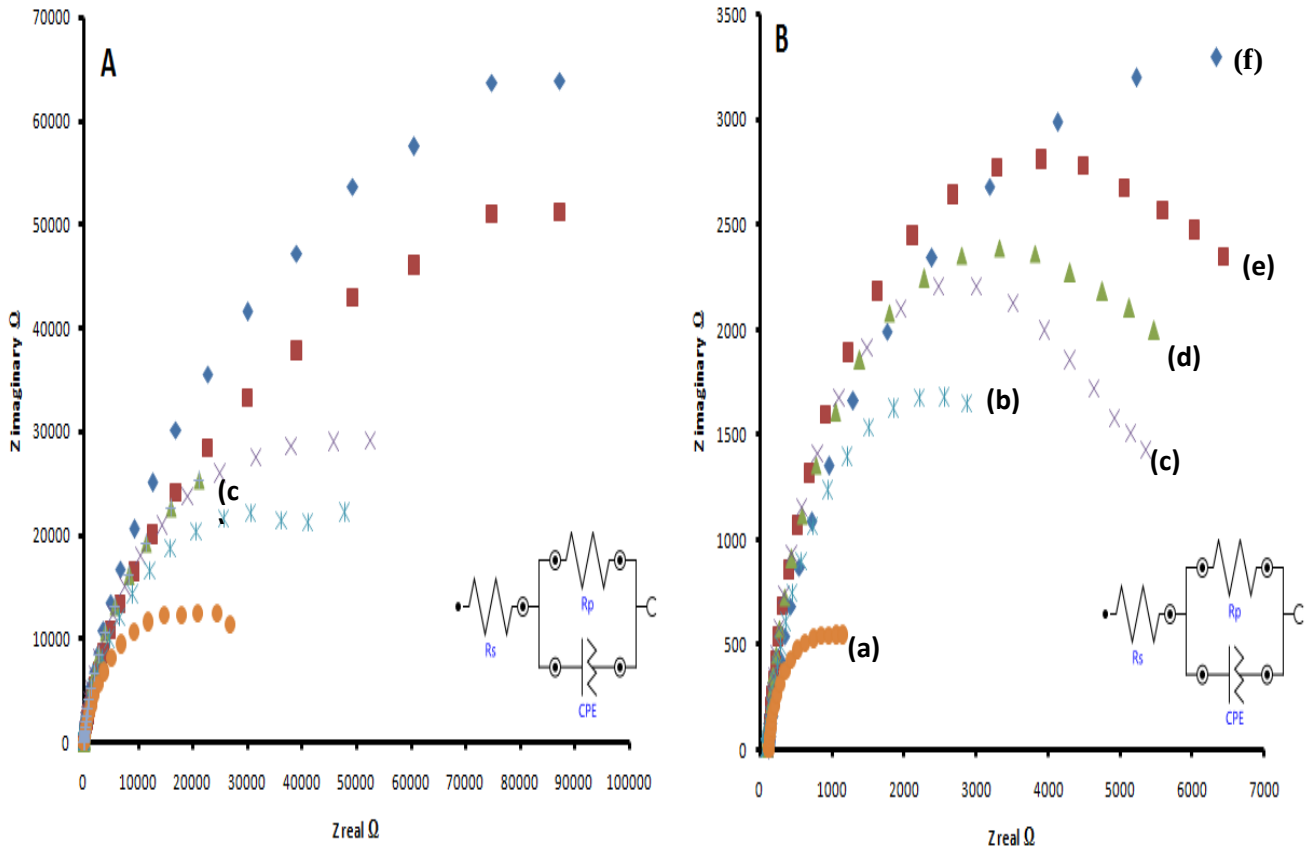

Fig 4. 10 Cyclic Voltammograms (A) Dopamine (B)Ascorbic Acid of bare (f) Fe_2O_3NPs -GCE (e), NiTAPc-GCE (d), NiTAPc-Fe_2O_3 NPs -GCE (c),NiTAPc-GONs-GCE b) and NiTAPc-GONs-Fe_2O_3NPs a) in 1mM dopamine and Ascorbic acid 0.1 M phosphate buffer (pH 7.0).

4.5 Kinetic analysis for Ascorbic and Dopamine

The influence of the scan rate on the electrochemical oxidation of ascorbic acid and dopamine (Fig 4.11 A and B) respectively at NiTAPc-GONs-Fe_2O_3NPs -GCE were investigated using cyclic voltammetry. The results showed that on increasing the scan rates the oxidation potential of ascorbic acid and dopamine shifts to more positive values confirming the kinetic limitation of the electrochemical reaction. Moreover, a plot of peak current (Ipa) versus the square root of the scan rate (√v) (Fig 4.11 A and B) Inset for NiTAPc-GONs-Fe_2O_3-GCE the range of 50-350 mV/s was found to be linear following the linear regression equation

Ipa (A) = 2.202 (mV/s) + 26.00 (R^2 = 0.999) Ascorbic Acid

Ipa (B) = 1.550 (mV/s) + 18.71 (R^2 = 0.996) Dopamine

Revealing that the electro-catalytic oxidation of ascorbic acid and dopamine at NiTAPc-GONs-Fe_2O_3 -GCE followed a diffusion controlled electron transfer process. The ΔEp increases at higher potential scan rates. This slight deviation from ideality may be due to
chemical interaction between DA and the composite. It was observed that DA anodic and cathodic peaks increase simultaneously with increase in scan rates from 50mV/s-350mV/s. As in Figure 4.11 (B), the anodic current is more pronounced than the reduction current, suggesting that the potential sweep favours electro oxidation of DA. This observed non-symmetrical forward and reverse peaks of DA in should perhaps not be surprising as other
works [17] have also observed the same and ascribed it to the working pH conditions.

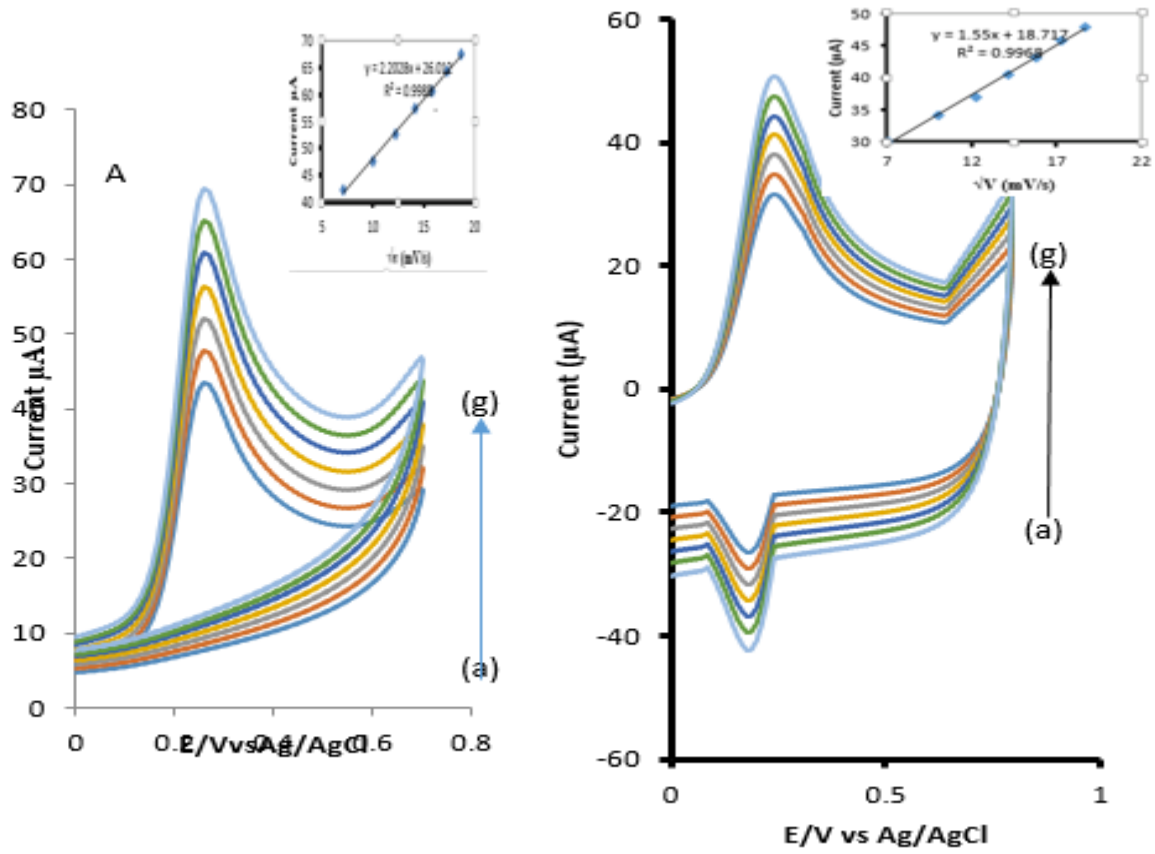

Fig 4. 11: Effect of scan rate on peak potentials and currents a) 50 mV/s, b) 100 mV/s, c) 150 mV/s, d) 200 mV/s, e) 250 mV/s, f) 300 mV/s and g) 350 mV/s on NiTAPc-GONS-Fe_2O_3NPs for (A) Ascorbic acid (B) Dopamine oxidation. Inset: plot of Current vs √v.

4.6 Tafel Slopes for ascorbic and dopamine

The value of Tafel slope can be obtained from the variation of Epa with v in voltammetric data through equation:

$$E_{pa} = {}^{b(\log v)}/_{2} + constant \qquad (4.1)$$

where b is the Tafel slope

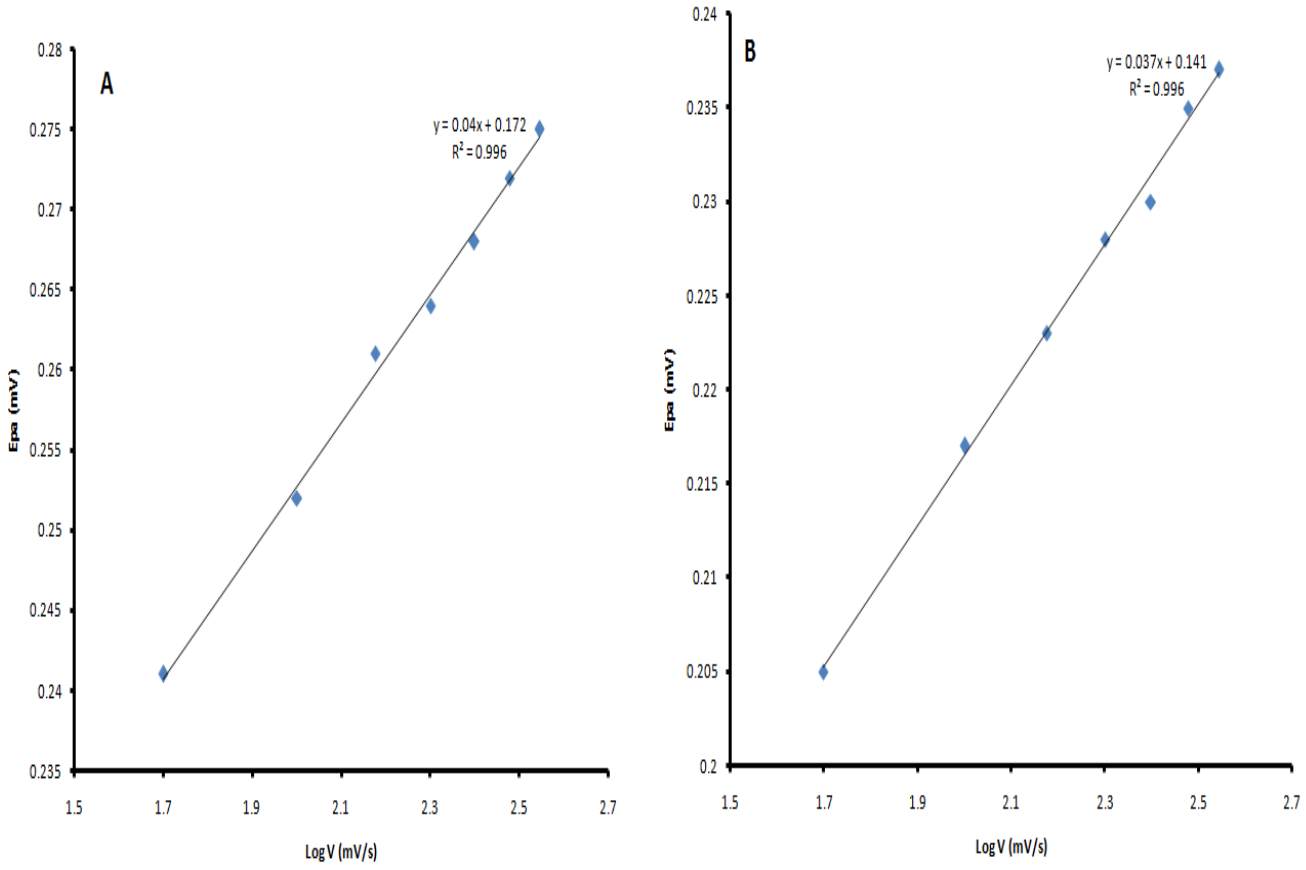

Fig 4. 12: Plot of potential versus log scan rate in 1 mM (A) Ascorbic acid and (B) Dopamine

The value of b is 2.303RT/(1-α)n_αF and Epc ,α, n_α and v are the oxidation peak potential ,electron transfer coefficient, number of electrons in the rate determining step and scan rate respectively. Tafel slope of 80 and 74 mV decade $^{-1}$ (2 × slope of plot was obtained for ascorbic and dopamine. The value of Tafel slope gives an idea about the number electrons transferred in the rate determining step [57]. From the Tafel plot, value of b for ascorbic acid where found to be 80 mV/decade and 74 mV/decade for dopamine at NiTAPc-GONS-Fe_2O_3NPs respectively. The values are within the usual range of 0.03-0.120 V indicating a strong binding interaction of the analyte and the catalyst.

4.7 Linear Sweep Studies

Linear sweep voltammetry (LSV) was done to show adsorption behaviour of NiTAPc-GONS-Fe_2O_3. Fig 4.13 shows LSV plots obtained after keeping the electrode in a stirred solution for 20 minutes to allow for adsorption.

Ipa = 35.15 [Dopamine] + 30.50 R^2 = 0.999

Ipa = 65.08 [$Ascorbic\ Acid$] + 38.05 R^2 = 0.994

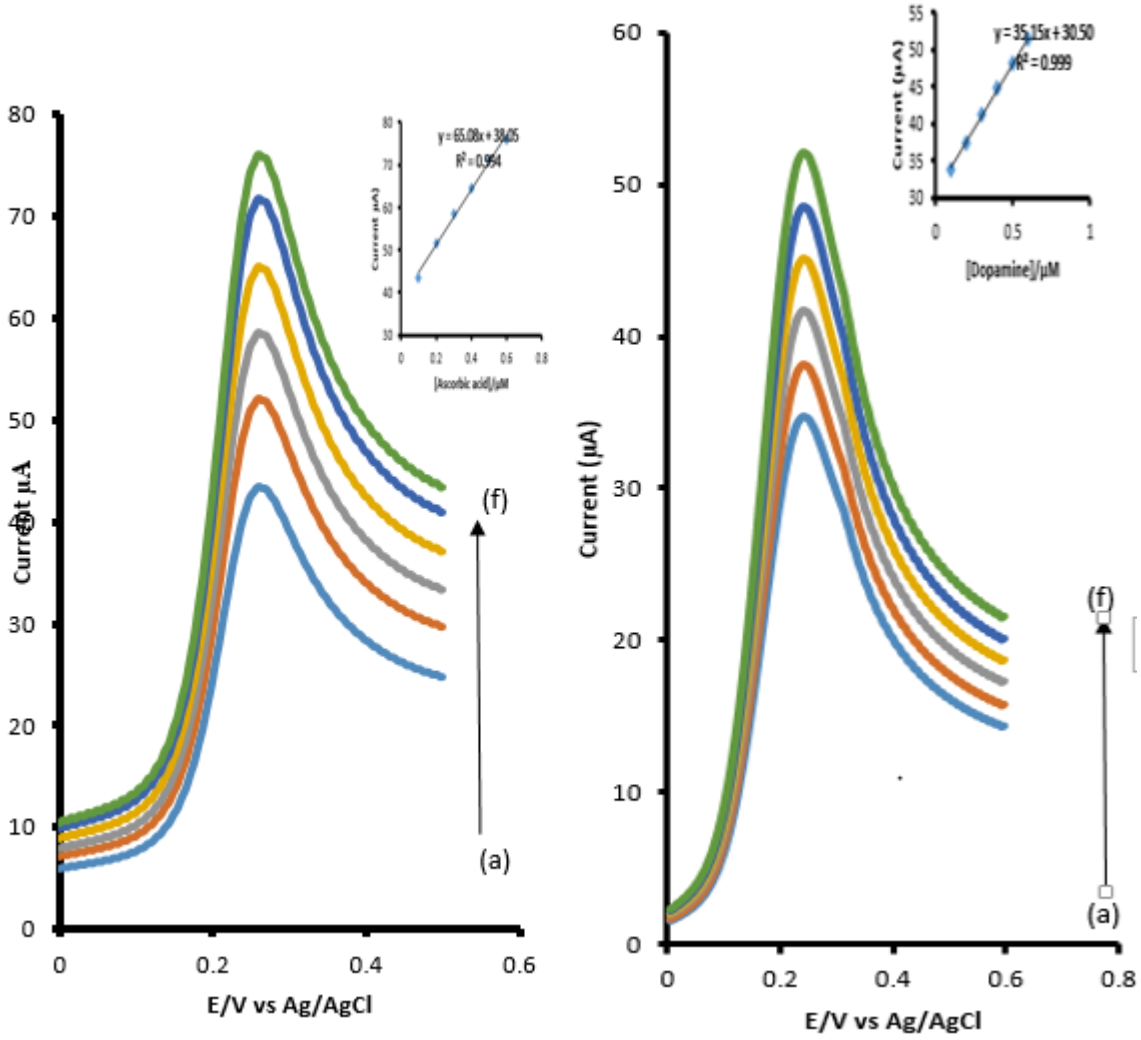

Fig 4. 13 Linear sweep Voltammograms (A) Ascorbic acid and (B) Dopamine (a) 10 µM, (b) 20 µM, (c) 30 µM (d) 40 µM, (e) 50 µM, 60 µM and 70 µM of Ascorbic acid and Dopamine concentrations in pH 7 PBS. Inset plot of Current vs. [Concentration].

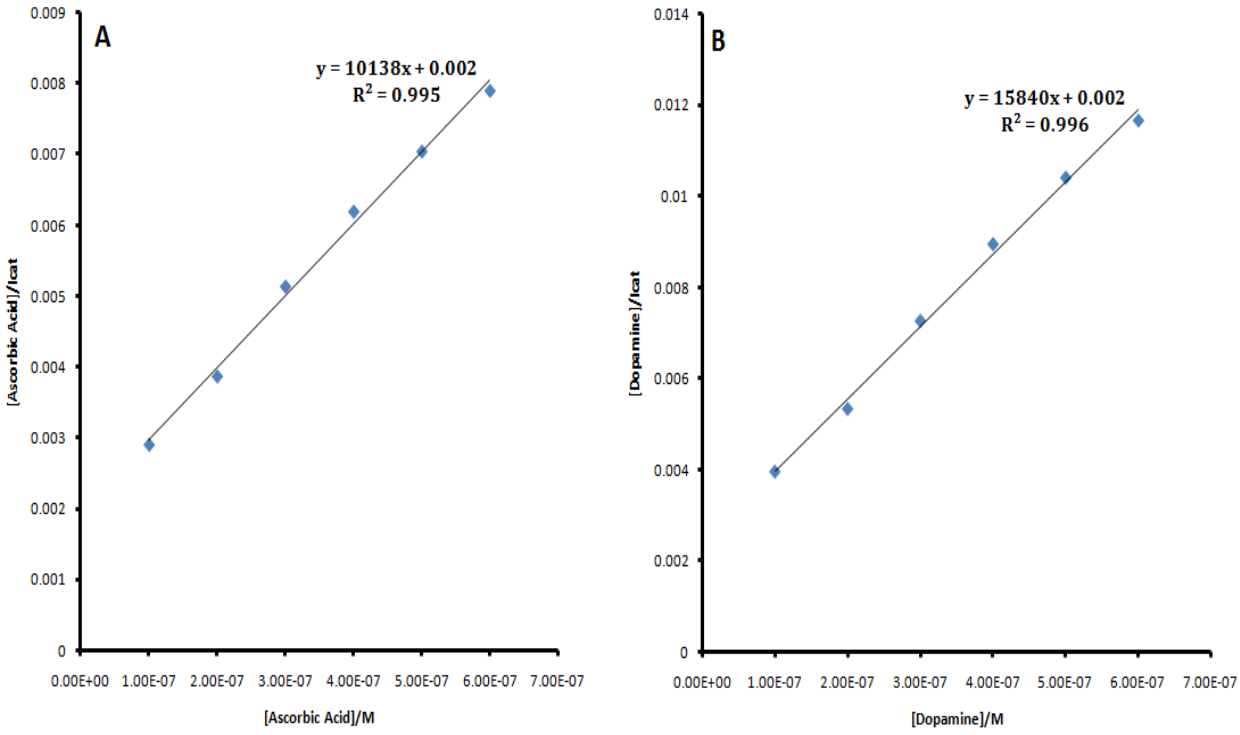

Fig 4. 14 Langmuir adsorption isotherm plot for (A) Ascorbic acid and (B) Dopamine on NiTAPc-GONS-Fe_2O_3NPs -GCE in a) 10 µM, (b) 20 µM, (c) 30 µM (d) 40 µM ,(e) 50 µM, 60 µM and 70 µM of ascorbic acid and dopamine concentrations in pH 7 PBS. Oxidation currents employed.

Applying the Langmuir adsorption theory (Eq 4.2), a plot of the ratio of Ascorbic Acid and dopamine concentration to catalytic current against concentration of Ascorbic acid and dopamine respectively gave a linear plot which can be interpreted as an adsorption controlled electrochemical process.

$$\frac{[analyte]}{Icat} = \frac{I}{\beta Imax} + \frac{analyte]}{Imax} \qquad (4.2)$$

Where [analyte] is the concentration of either dopamine or ascorbic acid where ß is the adsorption equilibrium constant, I_{max} is the maximum current and I_{cat} is the catalytic current. From the slope and the intercept of Fig 4.13 This value is in comparable to those reported elsewhere for high Tafel slopes [51].

$$\Delta G\circ = -RT\ ln\ ß \qquad (4.3)$$

Where R is the molar gas constant and T is room temperature

4.8 Differential Pulse Voltammetry

Under the optimal conditions, differential pulse voltammetry (DPV) was used to determine dopamine and ascorbic acid due to its higher sensitivity than cyclic voltammetry. Fig. 4.14 (A and B) shows the differential pulse voltammograms of different concentrations of dopamine and ascorbic acid in pH 7. As the DA concentration increased the current response did not increase any further, a phenomenon usually attributed to the saturation of the catalytic sites [22].

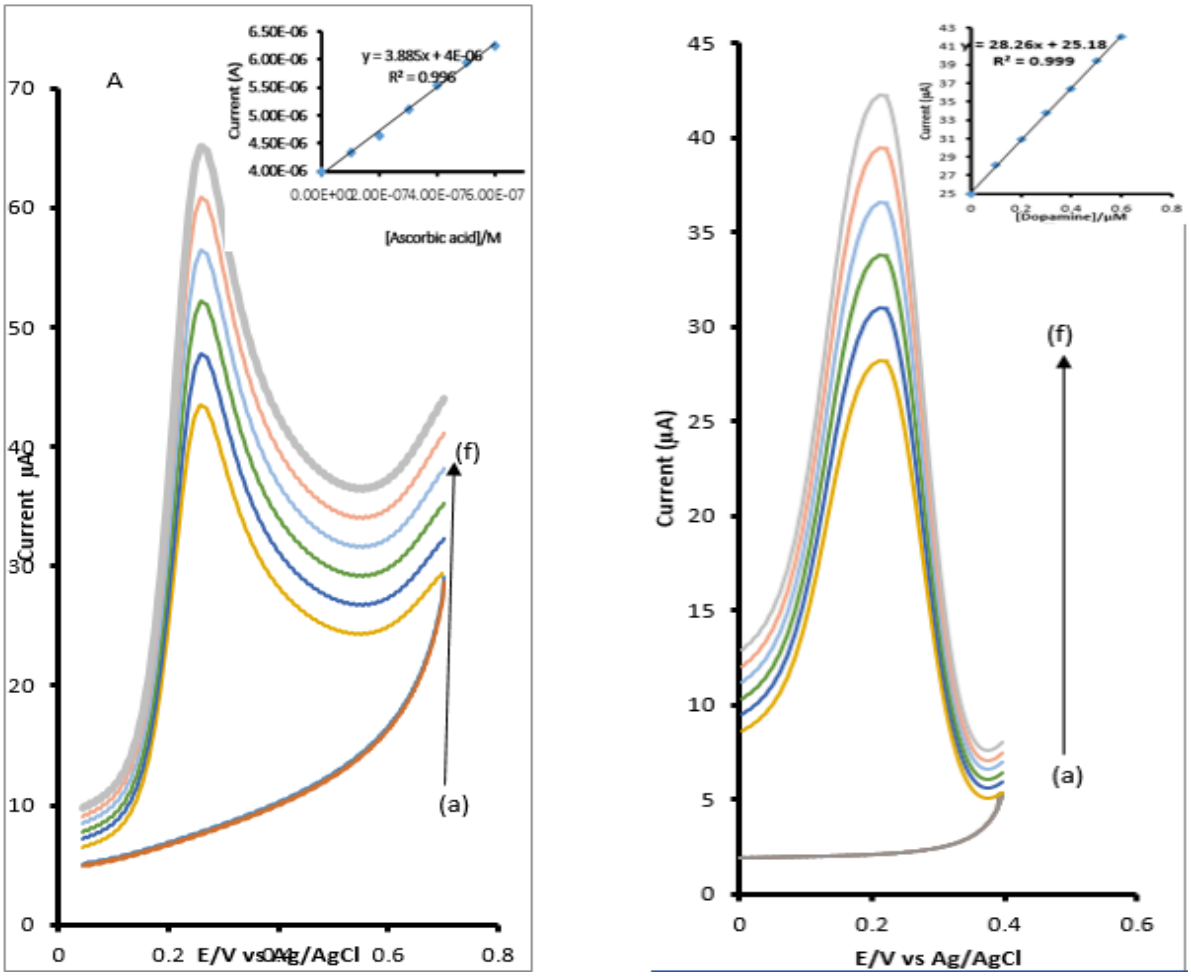

Fig 4. 15 (A and B) DPV for NiTAPc-GONS-Fe_2O_3NPs -GCE in: a) 0.2 µM, b) 0.4 µM, c) 0.6 µM, d) 0.8 µM, e) 1 µM, f) 1.2 µM, g) 1.4 µM, h) . Inset: Plot of Current vs [ascorbic acid]/[dopamine]

As can be seen in the inset of Fig. 4.15 (A) , the oxidation peak current was proportional to dopamine concentration in the range of between 0.2 and 1.2 μM with $r^2 = 0.99$. The limit of detection is equivalent to $3\sigma/s$ where $\sigma$is the standard deviation of the intercept and s is the slope of the calibration curve. LOD for dopamine was found to be 2.58×10^{-8} M. The LOQ ($10\sigma/s$) was found to be 6.8×10^{-8} M. The limit of detection of the electrode was much lower, and at about the same magnitude with values reported in literature [5] for some modified electrode towards DA electrocatalysis and detection. Dopamine is present at a micromolar concentration level in biological fluids thus the detection limit suggests that GONs- Fe_2O_3 hybrid might be suitable for the modification of ultra-microelectrodes for in-vivo detection of dopamine [21]. Fig 4.15 (B) The inset shows that the peak current varies linearly with ascorbic acid concentration between 0.2 and 1.2 mM with $r^2 = 0.999$. The limit of detection is equivalent to 3σ/s where σ is the standard deviation of the intercept and s is the slope of the calibration curve. LOD for ascorbic acid was found to be 8.6×10^{-8} M. The LOQ (10σ/s) was found to be 2.6×10^{-8} M.

4.9 Chronoamperometry Studies

Chronoamperometry data was used to determine catalytic rate constant for the oxidation of ascorbic acid and dopamine (Fig 4.16 A and B). Catalytic rate constants are a measure of how fast redox processes takes place at the electrode /analyte interface [60] The inset shows the linear relationship between current and concentration of AA, where current increases as the concentration of AA increases which is also true or dopamine. Fig 4.17 shows the plots of the ratio of catalytic currents and buffer currents (I_{cat}/I_{buff}) against square root of time within the rapid decay region. The plots gave linear relationships of the current ratios and the square roots of time.

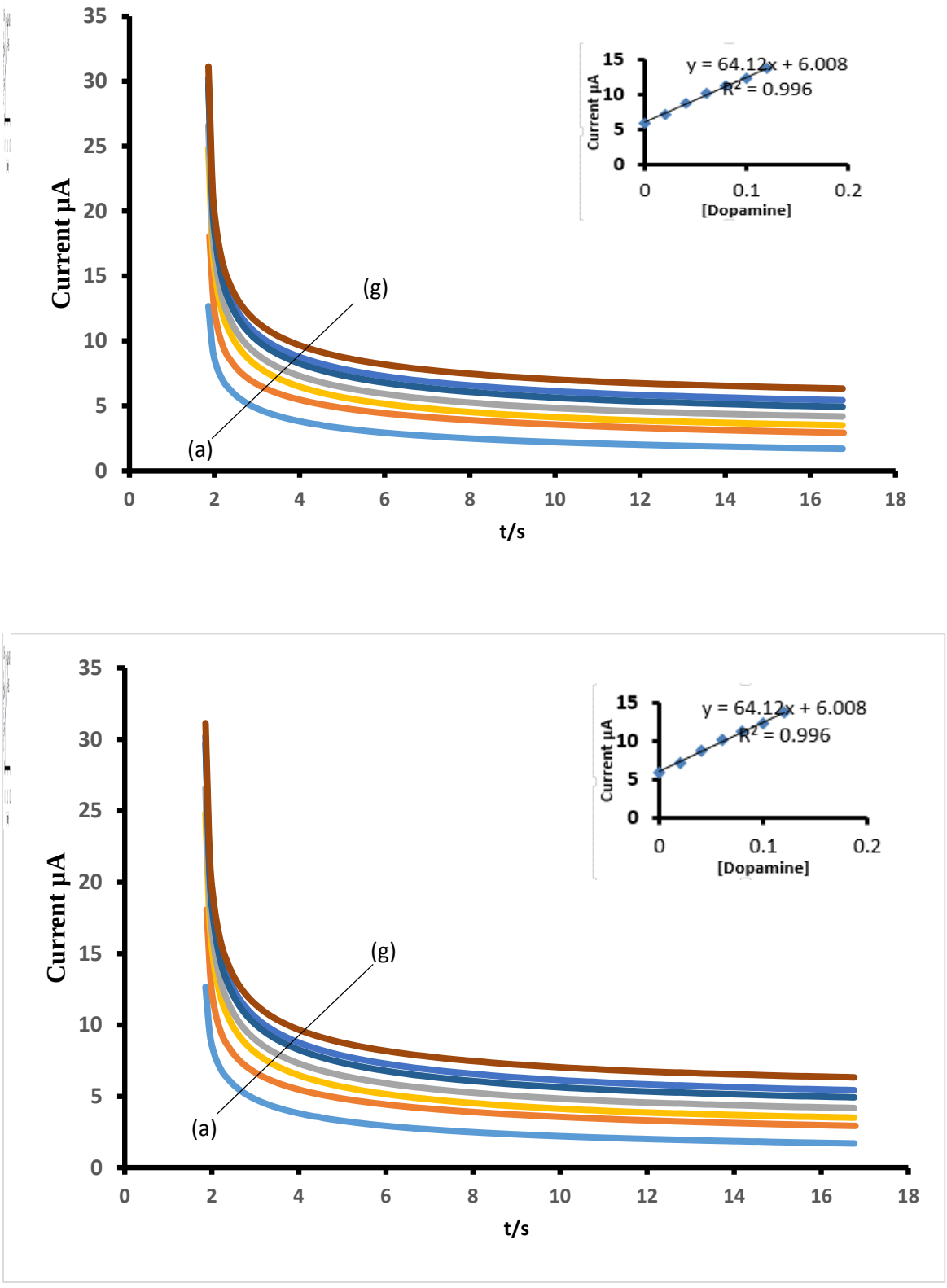

Fig 4. 16 : Chronoamperograms for different (A) Ascorbic acid and (B) Dopamine concentrations. In PBS pH 7 a), 0.02 µM b) , 0.04 µM c) , 0.06 µM d) , 0.08 µM e) , 0.1 µM f) and 0.12 µM g). *Inset* Current vs [ascorbic acid] (A) and [dopamine] (B)

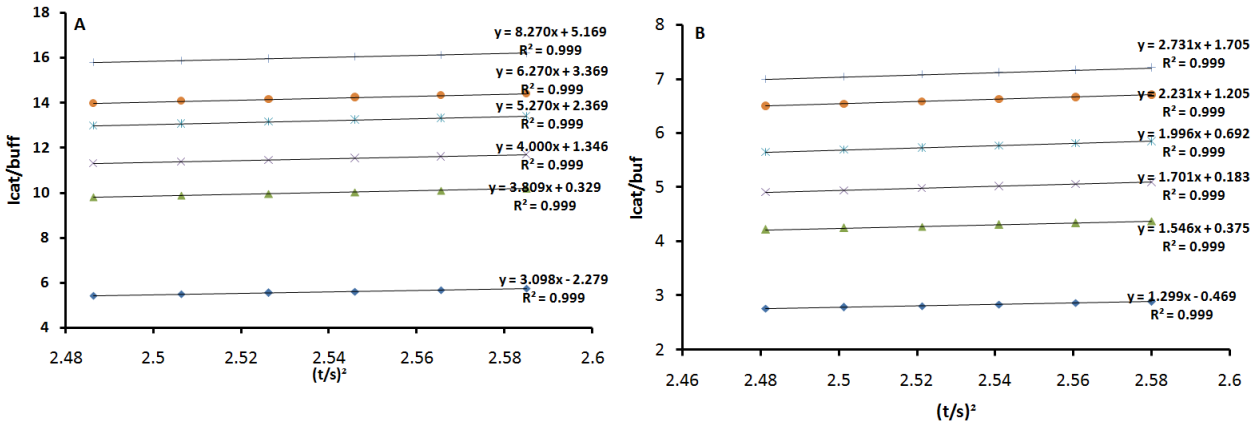

Fig 4. 17 Plots of Icat/Ibuf vs time (s) (A) Ascorbic Acid and (B) Dopamine

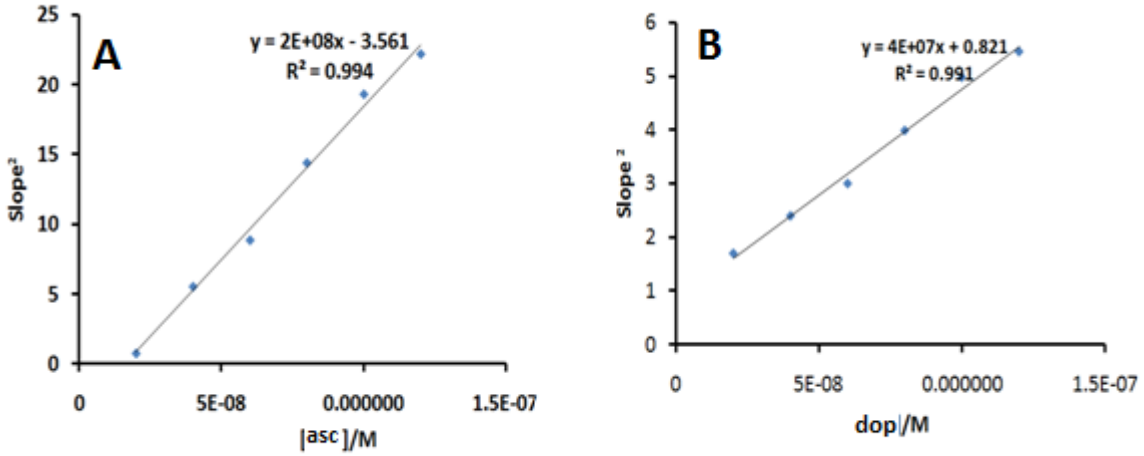

Fig 4.17 Plot of slopes2 vs. [Ascorbic Acid] (A) and (B) [Dopamine]

The rate constant for the detection of Ascorbic Acid and Dopamine was calculated using the equation:

$$\frac{I_{cat}}{I_{buf}} = \pi^{\frac{1}{2}}(kC_O t)^{1/2} \qquad (4.4)$$

Where Icat and Ibuf are currents in the presence and in the absence of ascorbic acid and dopamine, k is the catalytic constant ($M^{-1}s^{-1}$) for the ascorbic acid and dopamine oxidation and t is the time in seconds. Figure 4.17 (A and B). The slopes of Figure 4.16 A and B are equal to πk and this gives k values of 2.59 x 10^2 $M^{-1}s^{-1}$ for ascorbic acid and dopamine 1.56 x 10^2 $M^{-1}s^{1}$. The k values obtained for DA were in the same range as those reported for DA oxidation at aluminium electrode modified with nickel pentacyanonitrosylferrate films [31] and palladium hexacyanoferrate film. The difference in the k value is due to the different electrode modifier.

4.10 Stability studies for ascorbic and dopamine

Figure 4.18 A and B shows a 20 cycle continuous scan voltammograms for NiTAPc-GONs-Fe_2O_3NPs -GCE in 1 mM ascorbic acid and dopamine respectively. The stability of the modified electrode towards the detection of ascorbic acid indicated that the electrode remained almost constant during the experiment indicating that there was no signal loss for the sensor towards the detection of ascorbic acid. The electrode stability for the detection of dopamine also indicated no decrease in current. A percentage decrease of 1.95 % was observed from the first scan to the second scan. Drop in current is a passivation phenomenon and the rate at which the current drops is a measure of resistance to passivation of the electrode towards that analyte [67]. The percentage decrease of 1.95 % from the first scan to the second scan shows that the NiTAPc-GONS-Fe_2O_3NPs was not very stable.

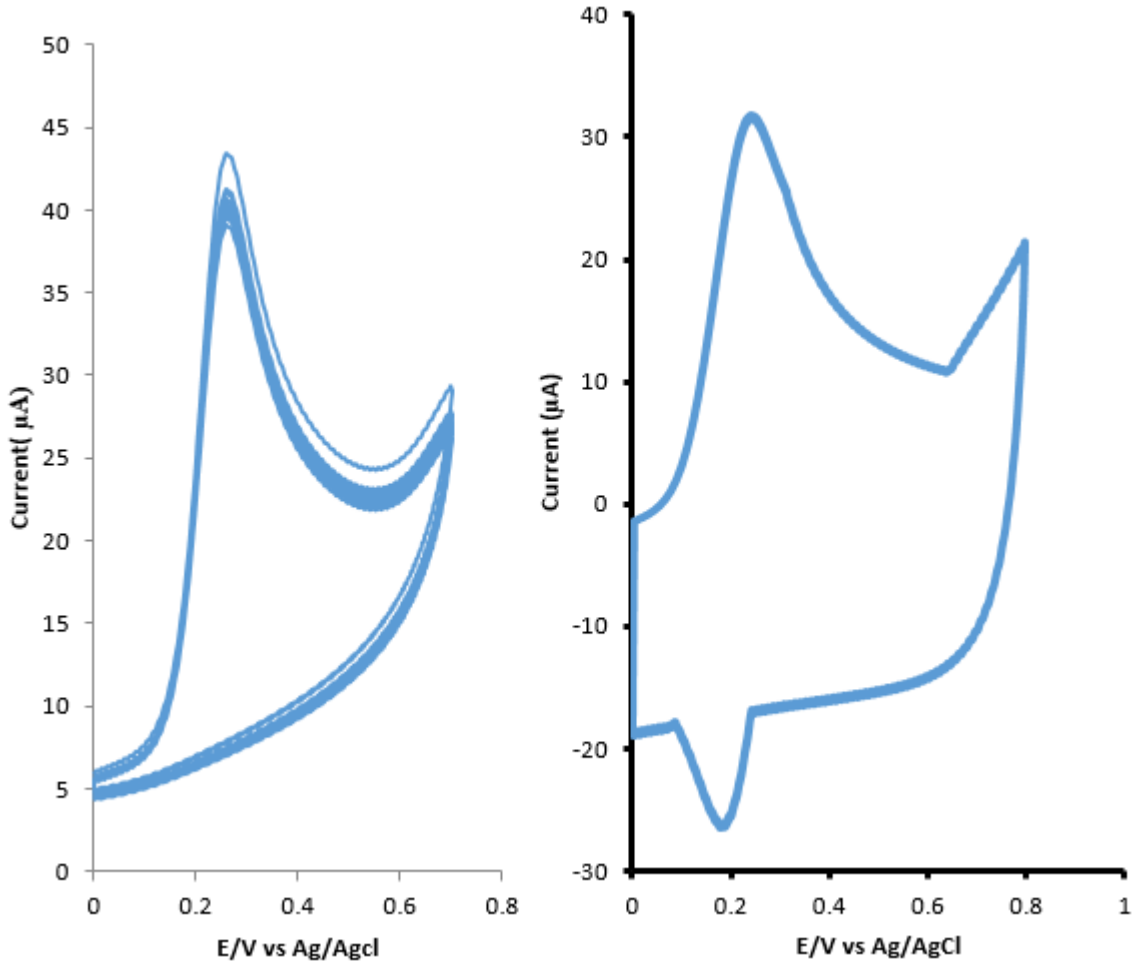

Fig 4. 18: A and B shows a 20 cycle continuous scan voltammograms for NiTAPc-GONS-Fe_2O_3NPs -GCE in 1mM Ascorbic acid and dopamine respectively.

4.11: Interference Studies

Equimolar concentration solutions of (A) dopamine and ascorbic acid, (B) dopamine and citric acid and (C) dopamine, ascorbic acid and citric acid were measured and ran separately and voltammograms were obtained and recorded. The oxidation peaks of dopamine, ascorbic acid and citric acid was found at 0.205 V, 0.266 V and 0.725 V respectively. From Fig 4.19 it was deduced that citric acid do not interfere with dopamine and ascorbic acid during determination. In fact, in all the concentrations of the DA studied there was no detectable interference of the AA and CA [5].

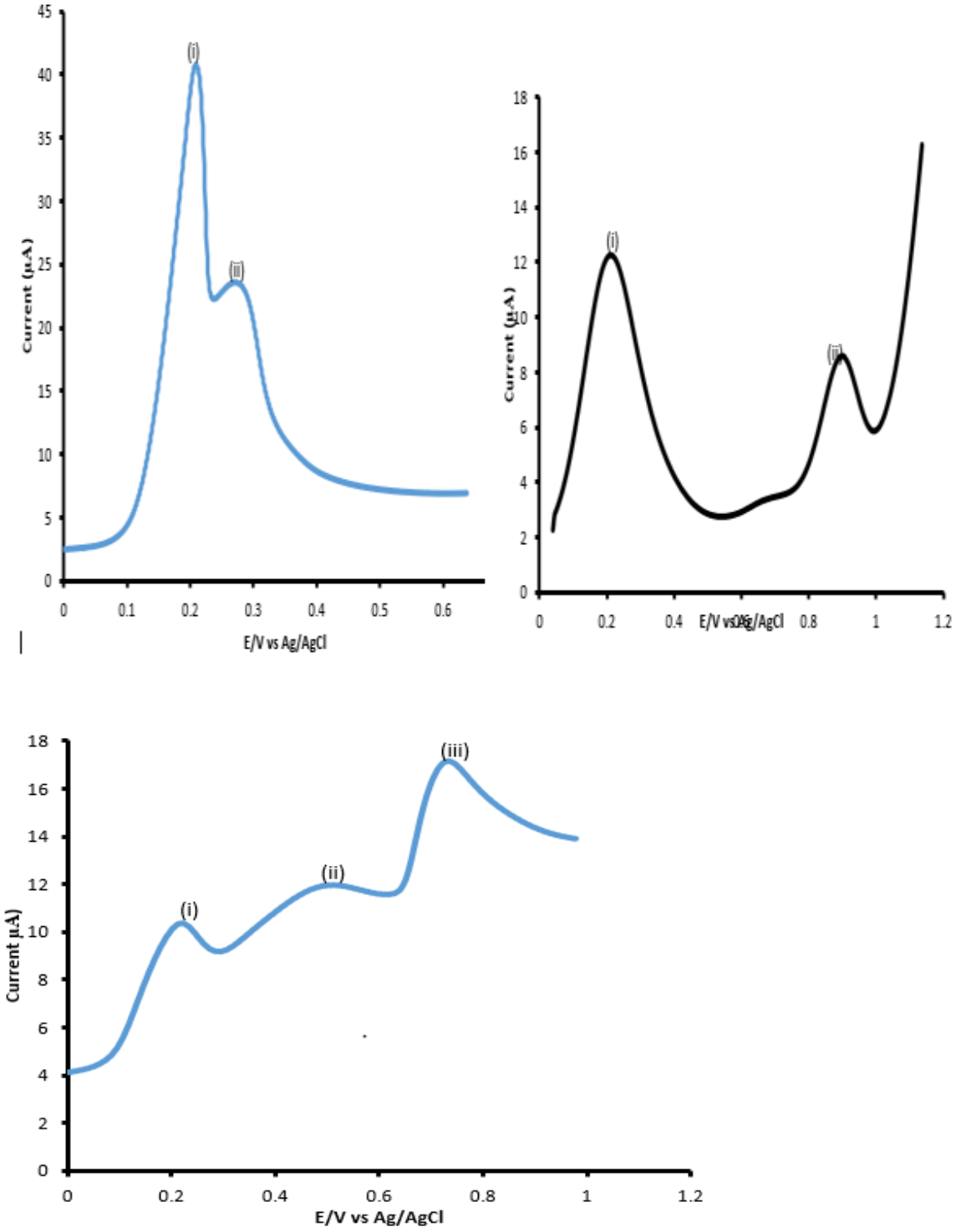

Fig 4. 19: Equimolar concentrations of dopamine and ascorbic acid (a) , dopamine and citric acid (b) , dopamine ,ascorbic acid and citric acid (c).

4.12 Simultaneous Detection of Ascorbic and Dopamine

Fig 4.20 shows the simultaneous cyclic voltammograms obtained on GONs-NiTAPc-Fe_2O_3-GCE composite film in equimolar solution of dopamine and ascorbic acid at different scan

rates. Fig 4.20 insets shows variation of peak intensities as a function of $v^{1/2}$ the equations fit well to a straight line. The equations are given below show that for the oxidation process they is mass transfer controlled oxidative electron transfer.

$\boldsymbol{Ipa}$ = 2.066 $\boldsymbol{v}^{1/2}$ + 23.62 $\boldsymbol{R}^2$ = **0. 99**2 Dopamine

$\boldsymbol{Ipa}$ = 1.127 $\boldsymbol{v}^{1/2}$ + 14.5 $\boldsymbol{R}^2$ = **0. 9**91 Ascorbic Acid

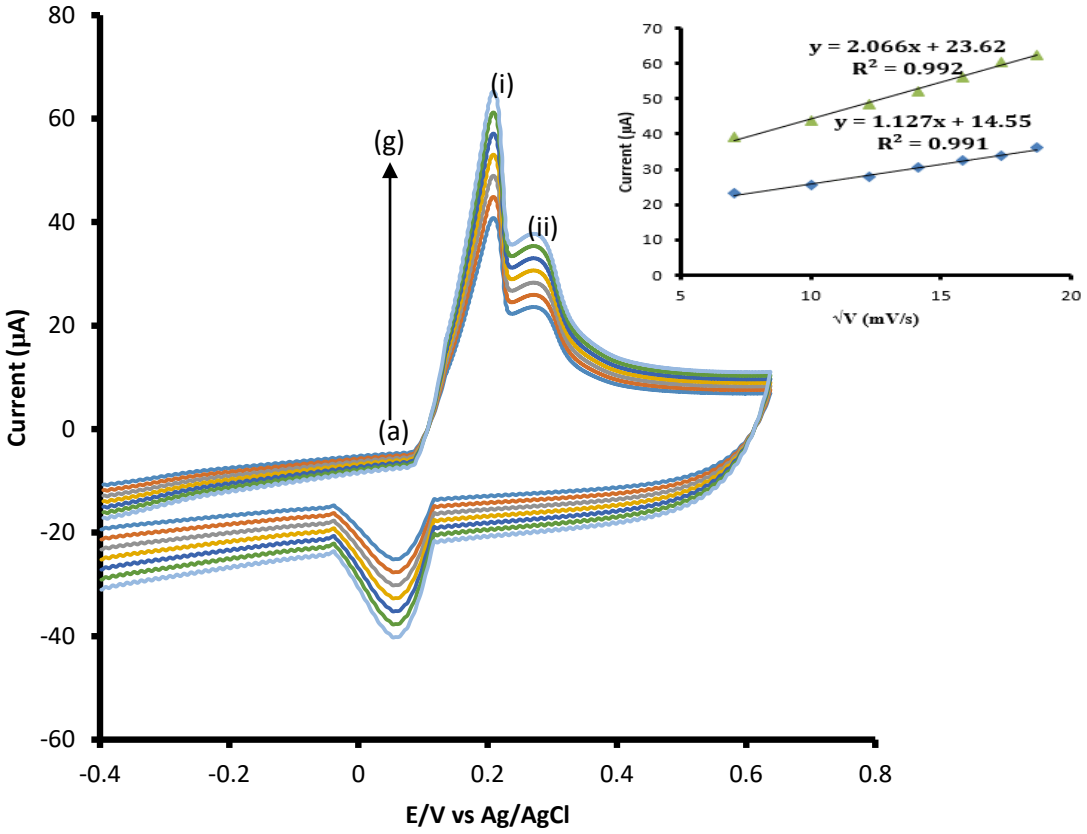

Fig 4. 20 : Simultaneous Cyclic voltammograms for the detection of equimolar solution of (i) ascorbic acid and (ii) dopamine at different scan rates(a) 50 mV/s, (b) 100 mV/s, (c) 150 mV/s, (d) 200 mV/s, (e) 250 mV/s, (f) 300 mV/s and (g) 350 mV/s on GONS-NiTAPc-Fe_2O_3-GCE. Insets show plot of Current vs.$v^{1/2}$ (scan rate).

On increasing the scan rates, the peak currents also increased. Meanwhile, the cathodic peak potentials showed a small shift and the peak-to-peak separation also increased. The anodic peak currents increased linearly with scan rates from 50 to 350 mV/s. A linear plot of current versus root of scan rate confirmed that the irreversible catalytic oxidation of ascorbic acid is diffusion controlled while dopamine is quasi reversible [55].

4.13 Simultaneous detection of dopamine and ascorbic acid

The simultaneous investigation was also done using differential pulse voltammetry. DPV was employed for its higher current sensitivity with better resolution. DPV was used to determine the linear ranges and the detection limit of dopamine and ascorbic acid at GONS-NiTAPc-Fe_2O_3-GCE. For simultaneous and quantitative determination of dopamine and ascorbic acid , DPV curves at different concentrations of dopamine were recorded in Fig. 4.21A, where ascorbic acid concentration was kept at 0.2 μM The inset shows that the peak current varies linearly with dopamine concentration between 0.2 and 1.2 μM with $r^2 = 0.993$. Importantly, the anodic peak current of ascorbic acid is almost uninfluenced by the increase of dopamine concentration, suggesting that oxidations of dopamine and ascorbic acid at the GONS-NiTAPc-Fe_2O_3-GCE are independent of each other [65]. With the DPV technique the detection limit of dopamine is 1.582×10^{-8} M in the presence of 0.2 μM ascorbic acid interference (S/N = 3) and limit of quantification was calculated to be 4.55×10^{-8} M (S/N = 10) . Fig. 4.21 B presents DPV responses at different concentrations of ascorbic acid while dopamine is kept constant at 0.2 μM. Similar to the scenario in Fig.4.21 A, the anodic peak current of dopamine stays almost constant as ascorbic acid concentration is increased gradually, further confirming that this modified electrode can be employed for simultaneous determination of dopamine and ascorbic acid. The inset in Fig. 4.21 illustrates that the peak current increases linearly with ascorbic acid concentration between 0.2 and 1.2 μM with $r^2 = 0.998$. In the presence of ascorbic acid, the

low limit is 1.162 x 10^{-7} M for ascorbic acid (S/N = 3) and limit of quantification was 3.52 x 10^{-7}M (S/N = 10).

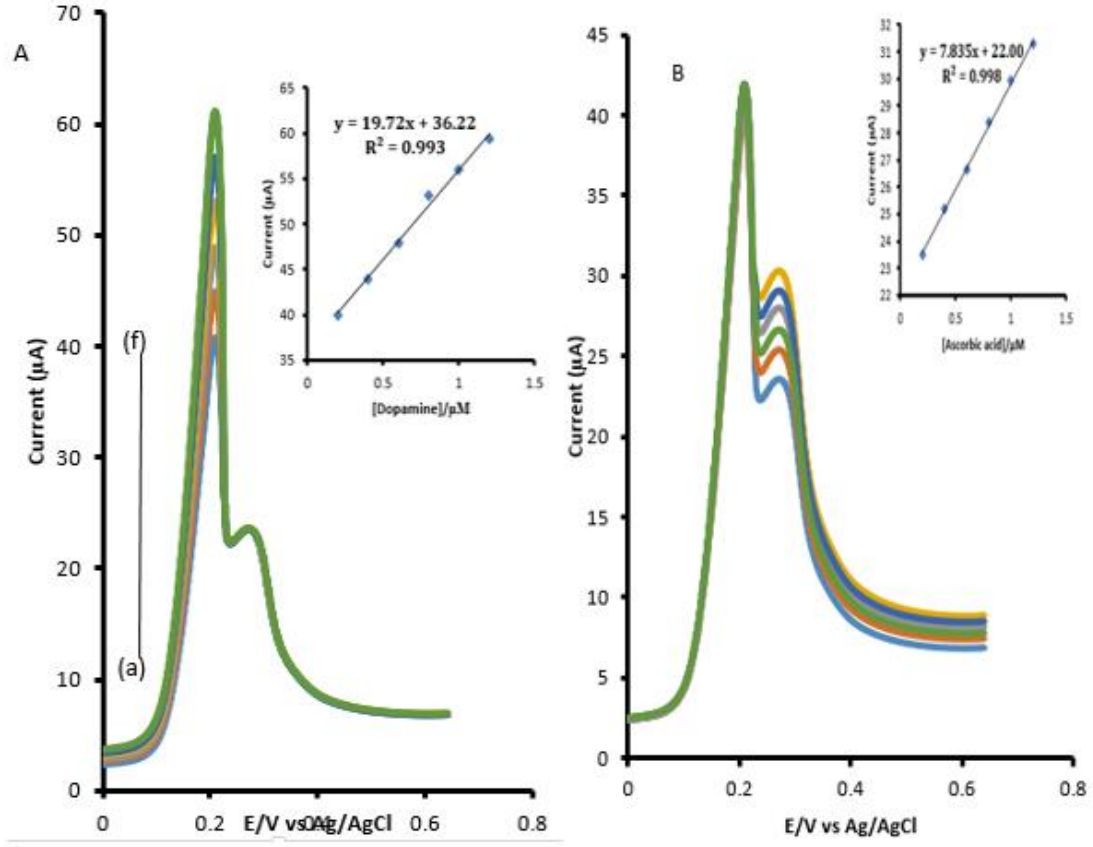

Fig 4. 21 Simultaneous DPV for (A) Dopamine and (B) Ascorbic Acid at GONS-NiTAP-Fe_2O_3-GCE in: a) 0.2 µM, b) 0.4 µM, c) 0.6 µM, d) 0.8 µM, e) 1 µM and f) 1.2 µM Inset: Plot of Ipa vs [dopamine]/ [ascorbic acid]

The effect of increasing concentration was investigated on GONs-NiTAPc-Fe_2O_3-GCE for the simultaneous determination of ascorbic acid and dopamine. As shown in Figure 4.21 two well distinguished oxidation peaks are observed, indicating that the catalytic reactions of dopamine and ascorbic acid at GONs-NiTAPc-Fe_2O_3-GCE occur independently. It appears that the peak corresponding to the oxidation of dopamine remains unaltered even if the concentration of AA greater than that of dopamine. This shows once again that there is no electrocatalytic effect of

AA on dopamine when these two molecules are present in solution [25]. The oxidation peak currents of Dopamine and ascorbic acid increase linearly with their concentration in the range m 0.2 – 1.2 µM.

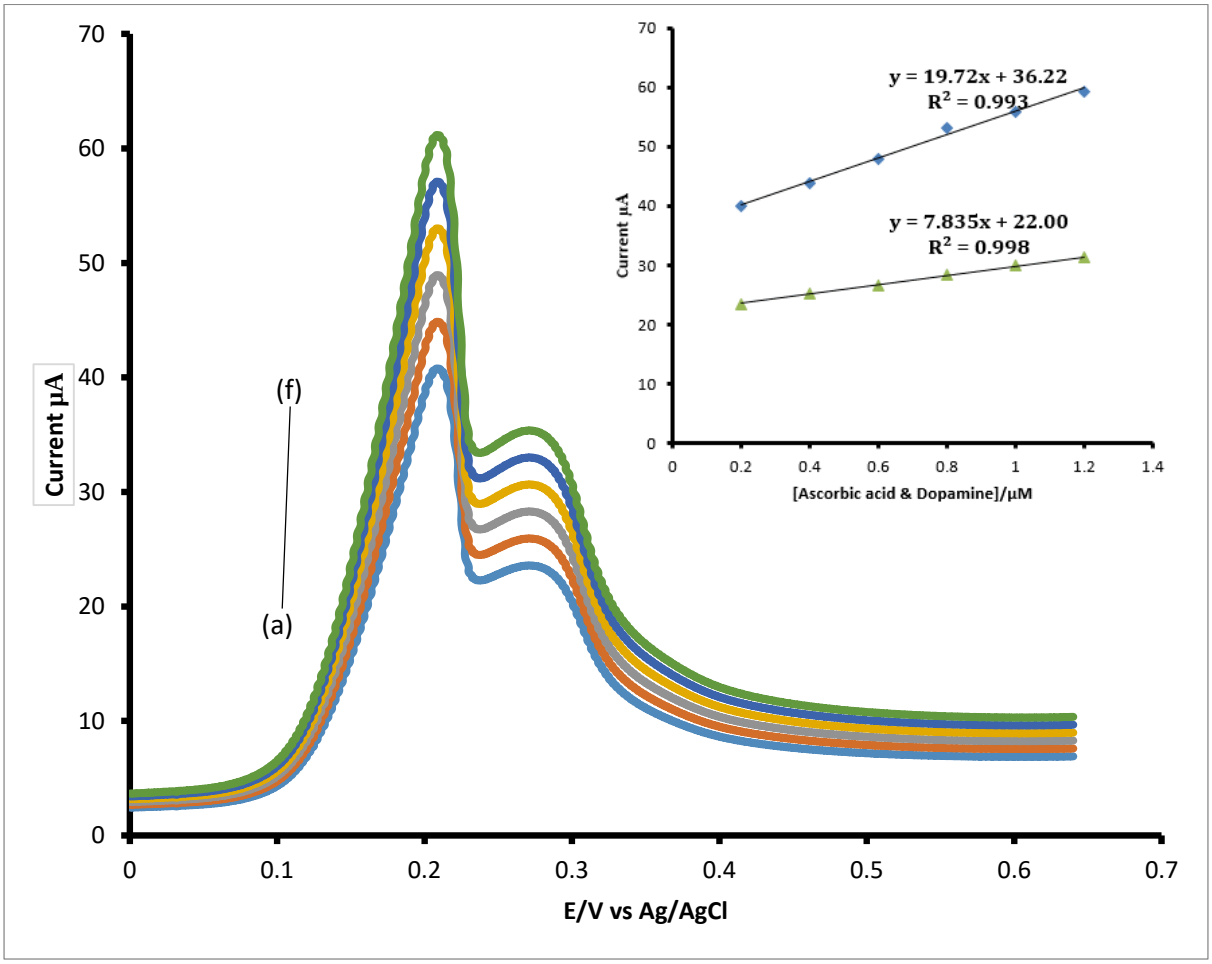

Fig 4.21 Simultaneous DPV for Dopamine and Ascorbic Acid at GONS-NiTAPc-Fe_2O_3-GCE in: a) 0.2 µM, b) 0.4 µM, c) 0.6 µM, d) 0.8 µM, e) 1 µM and f) 1.2 µM. Inset: Plot of Ipa vs [dopamine]/ [ascorbic acid]

The regression equations are given below:

Ipa (A) = 19.72 C + 36.22 R^2 = 0.993 Ascorbic acid

Ipa (B) = 7.835 C + 22.00 R ^{2} = 0.998 Dopamine

It was cited that for a given concentration of DA, a comparatively large oxidation current was noticed in the presence of AA at conventional electrodes [17]. This is due to the fact that oxidation product of DA, dopamine-o-quinone, catalytically reacts with AA and reduces the dopamine-o-quinone back to DA [32]. Therefore, the concentration of DA could not be determined accurately in the presence of AA. However, in the present investigation, the oxidation potential of DA are almost the same in the presence or absence of AA. NiTAPc-GONs-Fe_2O_3-GCE exhibited the bigger response for the oxidation of DA compared to AA, the oxidation of AA was effectively suppressed. AA had nearly no interference for the determination of DA. Thus the results demonstrate that ascorbic acid and dopamine can be selectively determined without interference from each other.

4.14 Stability Studies

The stability of GONs-NiTAPc-Fe_2O_3-GCE under working conditions was investigated by cyclic voltammetry by continuous scanning the electrode for 20 cycles in the presence of equimolar solutions of ascorbic acid and dopamine .Fig 4.22 indicates the response stability of GONs-NiTAPc-Fe_2O_3-GCE to equimolar solutions of ascorbic acid and dopamine solution at a scan rate of 0.1 V/s and a potential range of -0.4 to 0.6 V .As shown the anodic peak current of both ascorbic acid and dopamine oxidation remained almost constant during the experiment indicating that the was no signal loss for the sensor. This also confirmed the reusability of the electrode.

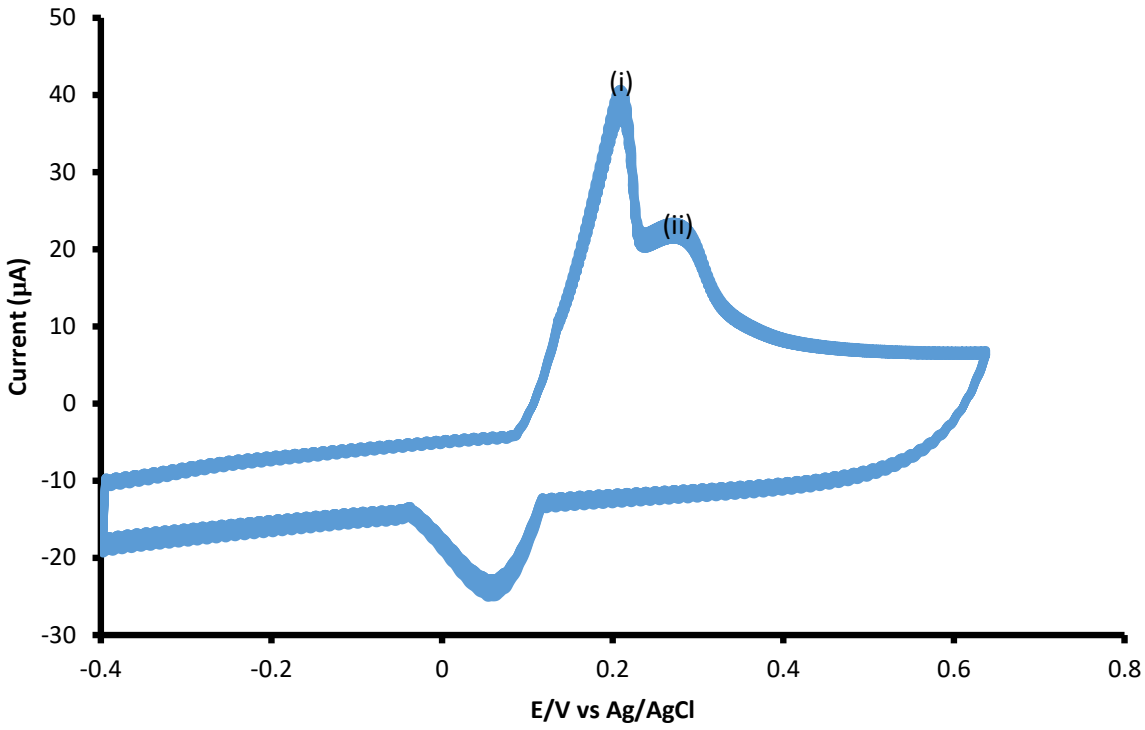

Fig 4. 22 Continuous cyclic voltammetric evolutions for equimolar solution of ascorbic acid (i) and (ii) dopamine generated on GCE modified with GONS-NiTAP-Fe_2O_3-GCE NGO. Scan rate = 100 mV/s. pH 7 PBS

4.15 Reproducibility

To evaluate the reproducibility of GONs-NiTAPc-Fe_2O_3 modified GCE for the determination of dopamine and ascorbic acid (Fig 4.23 A and B) respectively, we take successive measurements of differential pulse voltammetry in 0.1 M PBS pH 7 containing 1mM dopamine and ascorbic acid for 5 times .The modified surface area provided better reproducibility as indicated by the slight decrease in the peak current after washing the electrode and sonicating it in ethanol. The calculated percentage signal loss for the electrode was 1.85 % and 1.97 % respectively, these values were below 5 % and this indicated good repeatability of the modified electrode [60].

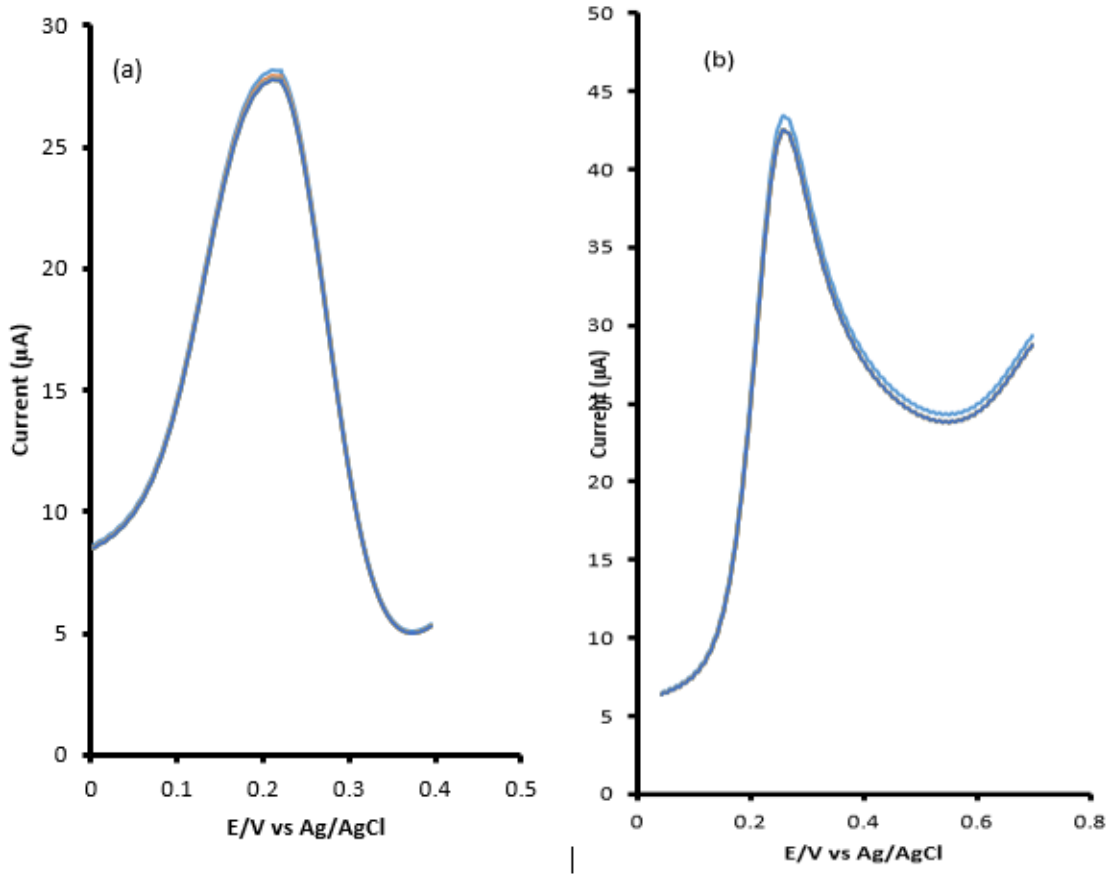

Fig 4.23: Reproducibility of a) dopamine and b) ascorbic acid in 0.1M PBS at pH 7.

Chapter 5

Conclusion and Recommendations

5.0 Introduction

This chapter serves to summarize this research, it is a brief summary of the work done and results obtained. It gives the recommendations that can be used for further studies in the area of interest.

5.1 Conclusion

In this research a sensor based on GONS-NiTAPc-Fe_2O_3 was fabricated and its characteristics were comprehensively studied. Both CV and DPV techniques were employed in the

simultaneous determination of Dopamine and ascorbic acid in the PBS of pH 7 at the modified electrode. The modified electrode exhibited good stability and sensitivity. Well defined and discrete voltammetric oxidation peaks were observed. The electrode showed good reproducibility with less than 5% signal loss and high sensitivity towards the detection of ascorbic and dopamine. The detection limits (LOD) of dopamine and ascorbic at the GONS-NiTAPc-Fe_2O_3-GCE were found to be and respectively. Moreover, the possible interference of dopamine and ascorbic was also studied using the modified electrode and the proposed method has been practically and successfully shown that citric acid cannot interfere with dopamine and ascorbic towards the simultaneous detection.

5.2 Recommendations

Further studies can still be done in order to enhance the performance of the developed sensor. This can be achieved by incorporating also different metals within the composite of PCs for example Cobalt and Copper this metals have high catalytic properties hence they can increase the rate of dopamine and ascorbic oxidation .Also the electrodes can further be applied towards multiple detection of ascorbic acid ,uric acid and dopamine .Further characterization techniques such as SEM ,TEM and XRD can also be employed to determine the particle distribution ,morphology and particle size . Enhancement of the chemical sensor can be done to further improve its already good sensitvity, selectivity and stability. This can be done by using nanosized metallo phthalocyanines, which can greatly improve the catalytic behaviour of phthalocyanines. The reduction in size, increases the surface area of the metallo phthalocyanines which in turn improve their catalytic behaviour.

REFERENCES

[1] Z.-H. Sheng, X.-Q. Zheng, J.-Y. Xu, W.-J. Bao, F.-B. Wang, and X.-H. Xia, "Electrochemical sensor based on nitrogen doped graphene: Simultaneous determination of ascorbic acid, dopamine and uric acid," *Biosens. Bioelectron.*, 34, 125–131,2012.

[2] H. Li., "An electrochemical sensor for simultaneous determination of ascorbic acid, dopamine, uric acid and tryptophan based on MWNTs bridged mesocellular graphene foam nanocomposite," *Talanta*, 127, 255–261, 2014.

[3] J. Kim, "Selective detection of dopamine in the presence of ascorbic acid via fluorescence quenching of InP / ZnS quantum dots," *Electrochimica Acta* ,12,113–119, 2015.

[4] M. Ben Atyah, "Selective and sensitive detection of dopamine in the presence of ascorbic acid and uric acid at a Sonogel-Carbon L-Histidine modified electrode," *Sens. Actuators B Chem.*, 9, 66–76, 2018.

[5] W. Wang., "Sensitive Electrochemical Detection of Dopamine With a Nitrogen-doped Graphene Modified Glassy Carbon Electrode," *Arab. J. Chem.*, 89, 3,323–330, 2016.

[6] W. Cai, J. Lai, T. Lai, H. Xie, and J. Ye, "Controlled functionalization of flexible graphene fibers for the simultaneous determination of ascorbic acid, dopamine and uric acid," *Sensors Actuators B Chem.*, 224, 225–232,2016.

[7] B. Paulchamy, G. Arthi, and L. Bd, "A Simple Approach to Stepwise Synthesis of Graphene Oxide Nanomedicine & Nanotechnology," *Anal. Chim. Acta*, 6,1–4, 2015.

[8] Q. Lai, S. Zhu, X. Luo, M. Zou, and S. Huang, "Ultraviolet-visible spectroscopy of graphene oxides," *AIP Adv.*, 2,146,2012.

[9] S. Laurent.,“Magnetic Iron Oxide Nanoparticles : Synthesis , Stabilization , Vectorization , Physicochemical Characterizations , and Biological Applications,” *Anal. Chim. Acta.*,7,2064–2110, 2008.

[10] D. Maity and D. C. Ã. Agrawal, “Synthesis of iron oxide nanoparticles under oxidizing environment and their stabilization in aqueous and non-aqueous media,” *Adv. Mater.*, 308, 46–55, 2007.

[11] T. Branch, C. E. Guide, and R. Desai, “Synthesis and characterization of iron oxide nanoparticles and their application in the treatment of industrial wastewater," *TrAC Trends Anal. Chem.*, 7, 1–3, 2009.

[12] H. Singh, J. Du, P. Singh, G. Tom, and T. Hoo, “Journal of Photochemistry & Photobiology , B : Biology Development of superparamagnetic iron oxide nanoparticles via direct conjugation with ginsenosides and its in-vitro study,” *J. Photochem. Photobiol. B Biol.*,185,100–110, 2018.

[13] S. Arslan, “Phthalocyanines : Structure , Synthesis , Purification and Applications,” *Electroanalysis*,6,188–197, 2016.

[14] U. Isci and N. N-bridged, “Novel N-bridged diiron phthalocyanine complexes : synthesis , characterization and application in oxidation,” *Anal. Chem.*2013.

[15] S. A. Priola, “Porphyrin and Phthalocyanine Antiscrapie Compounds,” *Science (80-.).*, 287,1503–1506,2000.

[16] N. Z. Raji and D. R. Stojakovi, “Journal of Coordination Synthesis and Characterization of Some Nitro-Substituted Phthalocyanines of Nickel (II), Cobalt (II) and Copper (II),” *J. Colloid Interface Sci.*,37–41,2013.

[17] S. Cao, R. Yuan, Y. Chai, L. Zhang, X. Li, and R. Chai, “Electrocatalytic Oxidation of

Ascorbic Acid on Modified Glassy Carbon Electrode and Its Analytical Application," *J. Electroanal. Chem.*, 223–227, 2006.

[18] S. B. A. Barros, A. Rahim, A. A. Tanaka, L. T. Arenas, R. Landers, and Y. Gushikem, "Electrochimica Acta In situ immobilization of nickel (II) phthalocyanine on mesoporous SiO 2 / C carbon ceramic matrices prepared by the sol – gel method : Use in the simultaneous voltammetric determination of ascorbic acid and dopamine," *Electrochim. Acta*, 87,140–147, 2013.

[19] T. Rattana, S. Chaiyakun, N. Witit-anun, N. Nuntawong, and P. Chindaudom, "Preparation and characterization of graphene oxide nanosheets," *Procedia Eng.*, 32, 759–764, 2012.

[20] S. Qi, B. Zhao, H. Tang, and X. Jiang, "Determination of ascorbic acid, dopamine, and uric acid by a novel electrochemical sensor based on pristine graphene," *Electrochim. Acta*,161, 395–402, 2015.

[21] J. P. Pessan., "Iron Oxide Nanoparticles for Biomedical Applications : A Perspective on Synthesis , Drugs , Antimicrobial Activity , and Toxicity," *Adv. Mater.*, 06, 1–18 2018.

[22] T.Bhengo,M.Moyo,M.Shumba and O.J Okonkwo,"SimultaneousOxidative determination of antibacterial drugs in aqueossolution using anelectrodemodified with MWCNT decorated with Fe $_2$O $_3$ nanoparticles," 2018.

[23] S. Khene, S. Moeno, and T. Nyokong, "Voltammetry and electrochemical impedance spectroscopy of gold electrodes modified with CdTe quantum dots and their conjugates with nickel tetraamino phthalocyanine," *Polyhedron*, 30, 2162–2170, 2011.

[24] K. Makgopa, P. M. Ejikeme, and K. I. Ozoemena, "Electrochimica Acta Graphene oxide-modi fi ed nickel (II) tetra-aminophthalocyanine nanocomposites for high-power

symmetric pseudocapacitor," *Electrochim. Acta*, 212, 876–882, 2016.

[25] A. S. Adekunle, B. O. Agboola, J. Pillay, and K. I. Ozoemena, "Electrocatalytic detection of dopamine at single-walled carbon nanotubes – iron (III) oxide nanoparticles platform Sensors and Actuators B : Chemical Electrocatalytic detection of dopamine at single-walled carbon nanotubes – iron (III) oxide nanoparticles," *Res. Chem. Intermed.*, 14, 68-88, 2010.

[26] I. G. Casella, "Electrooxidation of ascorbic acid on the dispersed platinum glassy carbon electrode and its amperometric determination in flow injection analysis," *Electroanalysis*, 8,128–134,1996.

[27] A. K. Baytak and M. Aslanoglu, "A novel sensitive method for the simultaneous determination of ascorbic acid, dopamine, uric acid and tryptophan using a voltammetric platform based on carbon black nanoballs," *Arab. J. Chem.*, 60,920-945,2018.

[28] P. Moyo, T. Mugadza, G. Mehlana, and U. Guyo, "Synthesis and characterization of activated carbon–ethylenediamine–cobalt(II) tetracarboxyphthalocyanine conjugate for catalytic oxidation of ascorbic acid," *Res. Chem. Intermed.*,42,6511–6529,2016.

[29] P. Gregory, "Industrial applications of phthalocyanines,"*Electrochimica Acta*, 437,432–437, 2000.

[30] W. Dieter, "Practical Applications of Phthalocyanines – from Dyes and Pigments to Materials for Optical , Electronic and Photo-electronic Devices ," *Electroanalysis*, 5,191–202, 2012.

[31] T. Mugadza and T. Nyokong, "Electrochemical, microscopic and spectroscopic characterization of benzene diamine functionalized single walled carbon nanotube-cobalt (II) tetracarboxy-phthalocyanine conjugates," *J. Colloid Interface Sci.*,354, 437–

447,2011.

[32] I. Distributions, C. Rager, G. Schmid, and M. Hanack, “Influence of Substituents , Reaction Conditions and Central Metals on the,” *Anal. Chem.*,1, 280–288, 1999.

[33] M. H. M. Khan, K. R. V. Reddy, and J. Keshavayya, “Green Chemistry Letters and Reviews Synthesis , characterizations and biological studies hydroxyphenylimino phthalocyanine complexes,” *Biosens. Bioelectron.*, 8253, 125-141,2009.

[34] I. Organic, “Structural studies in copper and nickel phthalocyanines," *Sens. Actuators B Chem.*, vol. 22,62-80,2006

[35] E. Kaya and M. Durmus, “Synthesis and spectral and thermal characterization of new metal-free and metallophthalocyanines : investigation of their photophysical , photochemical , and,” *RSC Adv*, 4,

1118–1134, 2014.

[36] B. O. Agboola, K. I. Ozoemena, and T. Nyokong, “Electrochemical properties of benzylmercapto and dodecylmercapto tetra substituted nickel phthalocyanine complexes : Electrocatalytic oxidation of nitrite, *Chem. Sci.*,2, 33-56,2012.

[37] M. D. Carvalho, F. Henriques, L. P. Ferreira, M. Godinho, and M. M. Cruz, “Journal of Solid State Chemistry Iron oxide nanoparticles : the Influence of synthesis method and size on composition and magnetic properties,” *J. Solid State Chem.*,201, 144–152, 2013.

[38] A. Ashori, H. Rahmani, and R. Bahrami, “Preparation and characterization of functionalized graphene oxide/carbon fiber/epoxy nanocomposites,” *Polym. Test.*,48, 82–88, 2015.

[39] J. M. Chem, “Journal of Materials Chemistry,” *Angew. Chem. Int. Ed.*, 5676–5683,

2012.

[40] A. Sharma., “Structural , electronic structure and antibacterial properties of graphene-oxide nano-sheets,” *Chem. Phys. Lett.*, 698, 85–92, 2018.

[41] H. Chen, S. Zhou, and L. Wu, “Porous Nickel Hydroxide − Manganese Dioxide-Reduced Graphene Oxide Ternary Hybrid Spheres as Excellent Supercapacitor Electrode Materials,” *Chem. Sci.*, 2, 12-33, 2014.

[42] M. Naseska and Z. Ljubljana, “Fourier Transform,Avtor : Mimoza Naseska,” *Science*, 112, 1–12, 2016.

[43] T. Woods, “Industrial Sample Analysis William Herschel,” *Fourier Transform Infrared Spectrosc.*, 50, 39-68, 2004.

[44] W. M. Doyle, “Principles and Applications of Fourier Transform Infra- red (FTIR) Process Analysis,” *Science*, 112, 23-45,2000.

[45] P. Praktikum and V. I. S. Spectroscopy, “UV / VIS Spectroscopy,” *Science*, 30, 1–11, 2017.

[46] V. Spectroscopy, “Ultraviolet - Visible Spectroscopy (UV),” *Characterization of Materials*, 1–7, 2009.

[47] M. Khan and B. Seminar, “Ultraviolet/Visible ,” *J. Phys. Chem. B*, vol. 10, 6-20, 2009.

[48] O. Compounds, “Spectroscopy of Organic Compounds,” *Int. J. Mol. Sci.*, 11, 1–36, 2006.

[49] D. Andrienko, “Cyclic Voltammetry,” *Modern Aspects of Electrochemistry*, 32, 2–12, 2008.

[50] G. Krishnan, “Chapter-I Introduction and Overview of Cyclic Voltammetry and Its

Theoretical," *Anal Methods*, 4, 1-8, 2002.

[51] T. Peik-See ,"Simultaneous Electrochemical Detection of Dopamine and Ascorbic acid using Iron oxide/Reduced Graphene Oxide Modified Glassy Carbon Electrode ," *Biosens.* Bioelectron, 34, 70–76, 2014.

[52] H. Nay-Ming ,C. Voltammetry, "Experiment 3 : Cyclic Voltammetry," *Int. J. Mol. Sci.*, 11, 5-122010.

[53] P. N. Mashazi, K. I. Ozoemena, and T. Nyokong, "Tetracarboxylic acid cobalt phthalocyanine SAM on gold : Potential applications as amperometric sensor for H 2 O 2 and fabrication of glucose biosensor," *Electrochimica Acta*, 98, 32–40,2012

[54] N. L. Pocard., "Doped Glassy Carbon : A New Material for Electrocatalysis," *Modern Aspects of Electrochemistry*, 2, 8,771–784, 1992.

[55] A. Pandikumar"Cyclic Voltammetric Study of ferrocyanide / ferricyanide Redox Couple," *Turk. J. Chem.*, 4,4–6,2000

[56] H. J. Kwon and E. Akyiano, "Simulation of cyclic voltammetry of ferrocyanide / ferricyanide redox reaction in the EQCM Sensor," *Anal. Methods*, 5, 2–6, 2011.

[57] Y. Zhu, "Experimental analytical electochemistry,Cyclic Voltammetry At Solid Electrodes," *Chem. Sci.*, 3,1–6,2009

[58] M. B. Grisham, "Methods o detect hydrogen peroxide in living cells: Possibilities and pitfalls," *Comp. Biochem. Physiol. Part A*, 1–10, 2013.

[59] D. O. F. Philosophy, "Electrochemical studies on modified electrodes," *Chem. Rec.*, 2,1-12, 1990.

[60] D. Version, "Surface modified electrodes :an exploration into preparation ,

characterization and possibilities," *Chem. Phys. Lett.*,4 ,53–56, 1983.

[61] U. Reaction, "Chemically Modified Electrodes Chapter 14," *J. Power Sources*, 156,142–150, 2012.

[62] S. V Aurobind, K. P. Amirthalingam, and H. Gomathi, "Sol-gel based surface modification of electrodes for electro analysis," *J. Phys. Chem.*121,1–7, 2006.

[63] A. J. Bard, "Chemical Modification of Electrodes," *Science*, 13, 302–304, 1983.

[64] C. I. Values, P. Electrochemistry, C. Elements, C. Equivalent, and C. Models, "Basics of Electrochemical Impedance Spectroscopy," *Science*, 1,306-312, 2000.

[66] N.Hassanzadeh and H. Reza Zane-Mehrjardi, "Selective Electrochemical Sensing of Dopamine and Ascorbic Acid using Carbon Paste Electrode Modified with Cobalt Schiff Base Complex and a surfactant," *J. Phys. Chem. B*, 23, 35–48,2017

[67] I. Electrochem, "Pulse Voltammetry Normal Pulse Voltammetry," *J Chem Soc Dalton Trans*, 8, 1485–1489 1980.

[68] R. Georgescu, C. Boscornea, I. Calinescu, and R. State, "Raman , IR and UV-Vis Spectroscopic Investigations of Some Substituted Phthalocyanines," *Electroanalysis*, 2 ,66–69, 2015.

[69] S. N. Alam, N. Sharma, and L. Kumar, "Synthesis of Graphene Oxide (GO) by Modified Hummers Method and Its Thermal Reduction to Obtain Reduced Graphene Oxide (rGO)*," *Graphene*, 06, 1–18, 2017.

[70] A. T. Chidembo, K. I. Ozoemena, B. O. Agboola, V. Gupta, G. Wildgoose, and R. G. Compton, "Nickel (II) tetra-aminophthalocyanine modified MWCNTs as potential nanocomposite materials for the development of supercapacitors †," *Electrochimica*

Acta,228–236, 2010.